



DUNN, J. L. RY  
NAVY SCHOOL  
TOWSON, MD. 21286 85943-8002











# NAVAL POSTGRADUATE SCHOOL

## Monterey, California



## THESIS

B246E

HOT-WIRE MEASUREMENTS OF COMPRESSOR  
BLADE WAKES IN A CASCADE WIND TUNNEL

by

Adem Baydar

March 1988

Thesis Advisor

Raymond P. Shreeve

Approved for public release; distribution is unlimited.

T238691





# REPORT DOCUMENTATION PAGE

1a Report Security Classification Unclassified			1b Restrictive Markings		
2a Security Classification Authority			3 Distribution Availability of Report Approved for public release; distribution is unlimited		
2b Declassification Downgrading Schedule			5 Monitoring Organization Report Number(s)		
4 Performing Organization Report Number(s)			7a Name of Monitoring Organization Naval Postgraduate School		
6a Name of Performing Organization Naval Postgraduate School		6b Office Symbol (if applicable) 31	7b Address (city, state, and ZIP code) Monterey, CA 93943-5000		
6c Address (city, state, and ZIP code) Monterey, CA 93943-5000			9 Procurement Instrument Identification Number		
8a Name of Funding Sponsoring Organization		8b Office Symbol (if applicable)	10 Source of Funding Numbers		
8c Address (city, state, and ZIP code)			Program Element No	Project No	Task No
			Work Unit Accession No		
11 Title (include security classification) HOT-WIRE MEASUREMENTS OF COMPRESSOR BLADE WAKES IN A CASCADE WIND TUNNEL					
12 Personal Author(s) Adem Baydar					
13a Type of Report Master's Thesis		13b Time Covered From To		14 Date of Report (year, month, day) March 1988	15 Page Count 58
16 Supplementary Notation The views expressed in this thesis are those of the author and do not reflect the official policy or position of the Department of Defense or the U.S. Government.					
17 Cosati Codes			18 Subject Terms (continue on reverse if necessary and identify by block number)		
Field	Group	Subgroup	thesis, word processing, Script, GML, text processing.		
19 Abstract (continue on reverse if necessary and identify by block number) A hot-wire system, with software designed for calibrating and taking data with single, double and triple hot-wire sensors separately, or three probes at once, was verified and used to make wake measurements downstream of a compressor stator blade in a cascade wind tunnel. Using a single hot-wire probe, velocity and turbulence data were obtained in the wake of the controlled-diffusion blade in order to verify LDV data taken in earlier studies. The tests were conducted at three inlet angles from near design incidence towards the expected stall condition at a Mach number of 0.25 and Reynolds number of about 700,000. Wake profiles were obtained from 0.08 to 0.2 chord lengths downstream of the blade. Good agreement was found with LDV measurements. Measurements at the highest incidence angle showed that the wake constituted one third of the flow and yet no separation occurred before the trailing edge on the suction side of the blade.					
20 Distribution Availability of Abstract <input checked="" type="checkbox"/> unclassified unlimited <input type="checkbox"/> same as report <input type="checkbox"/> DTIC users			21 Abstract Security Classification Unclassified		
22a Name of Responsible Individual Raymond P. Shreeve			22b Telephone (include Area code) (408) 625-9011		22c Office Symbol 67Sf

Approved for public release; distribution is unlimited.

Hot-Wire Measurements of Compressor  
Blade Wakes in a Cascade Wind Tunnel

by

Adem Baydar

1. Lieutenant, Turkish Air Force  
B.S., Academy of Air Force, 1983

Submitted in partial fulfillment of the  
requirements for the degree of

MASTER OF SCIENCE IN AERONAUTICAL ENGINEERING

from the

NAVAL POSTGRADUATE SCHOOL  
March 1988

## ABSTRACT

A hot-wire system, with software designed for calibrating and taking data with single, double and triple hot-wire sensors separately, or three probes at once, was verified and used to make wake measurements downstream of a compressor stator blade in a cascade wind tunnel. Using a single hot-wire probe, velocity and turbulence data were obtained in the wake of the controlled-diffusion blade in order to verify LDV data taken in earlier studies. The tests were conducted at three inlet angles from near design incidence towards the expected stall condition at a Mach number of 0.25 and Reynolds number of about 700,000. Wake profiles were obtained from 0.08 to 0.2 chord lengths downstream of the blade. Good agreement was found with LDV measurements. Measurements at the highest incidence angle showed that the wake constituted one third of the flow and yet no separation occurred before the trailing edge on the suction side of the blade.

## TABLE OF CONTENTS

I. INTRODUCTION .....	1
II. TEST FACILITY .....	3
A. CASCADE WIND TUNNEL .....	3
B. PROBES AND TRAVERSE ARRANGEMENT .....	3
C. AUXILIARY INSTRUMENTATION .....	3
III. HOT-WIRE SYSTEM .....	10
A. HARDWARE .....	10
B. SOFTWARE AND DATA ACQUISITION: .....	10
1. Calibration Program .....	10
2. Data Acquisition Program .....	11
3. Statistical Analysis Program .....	11
4. Spectrum Correlation Program .....	11
5. Traverse Table Control Program .....	12
6. Flow Field Plot program .....	12
IV. EXPERIMENTAL PROCEDURE .....	15
A. TEST SECTION SET UP AND ADJUSTMENTS. ....	15
B. SURVEY PROCEDURE .....	15
1. Probe Calibration .....	15
2. Surveys .....	16
a. Upstream Probe Survey .....	16
b. Downstream Probe Survey .....	16
C. PROGRAM OF MEASUREMENTS .....	16
V. RESULTS AND DISCUSSION .....	17
A. WAKE VELOCITY DISTRIBUTIONS .....	17
B. TURBULENCE INTENSITY DISTRIBUTIONS .....	26
VI. CONCLUSIONS AND RECOMMENDATIONS .....	34

APPENDIX A. TABULATED REDUCED DATA .....	35
APPENDIX B. CALCULATION OF DIMENSIONLESS PARAMETERS ....	44
LIST OF REFERENCES .....	45
INITIAL DISTRIBUTION LIST .....	46

## LIST OF TABLES

Table 1.	COORDINATES of the CD BLADE	3
Table 2.	GEOMETRICAL PARAMETERS of the CASCADE	3
Table 3.	NOMINAL TEST CONDITIONS	3
Table 4.	PROGRAM of MEASUREMENTS	16
Table 5.	WAKE DISTRIBUTION DATA at $\beta_1 = 40.0^\circ$ , $Y = 0.08c$	35
Table 6.	WAKE DISTRIBUTION DATA at $\beta_1 = 40.0^\circ$ , $Y = 0.123c$	36
Table 7.	WAKE DISTRIBUTION DATA at $\beta_1 = 40.0^\circ$ , $Y = 0.2c$	37
Table 8.	WAKE DISTRIBUTION DATA at $\beta_1 = 46.0^\circ$ , $Y = 0.08c$	38
Table 9.	WAKE DISTRIBUTION DATA at $\beta_1 = 46.0^\circ$ , $Y = 0.123c$	39
Table 10.	WAKE DISTRIBUTION DATA at $\beta_1 = 46.0^\circ$ , $Y = 0.2c$	40
Table 11.	WAKE DISTRIBUTION DATA at $\beta_1 = 48.0^\circ$ , $Y = 0.08c$	41
Table 12.	WAKE DISTRIBUTION DATA at $\beta_1 = 48.0^\circ$ , $Y = 0.123c$	42
Table 13.	WAKE DISTRIBUTION DATA at $\beta_1 = 48.0^\circ$ , $Y = 0.2c$	43



## LIST OF FIGURES

Figure 1.	Cascade Wind Tunnel Schematic . . . . .	4
Figure 2.	Cascade Test Section Instrumentation and Physical Dimensions. . . . .	5
Figure 3.	View of the Cascade Wind Tunnel and Dual-Probe Traverse . . . . .	8
Figure 4.	Probe Survey Stations. . . . .	9
Figure 5.	Hot-Wire System Hardware . . . . .	13
Figure 6.	Software Flow Chart . . . . .	14
Figure 7.	Wake Velocity Distribution at $\beta_1 = 40.0^\circ$ . . . . .	19
Figure 8.	Wake Velocity Distribution at $\beta_1 = 46.0^\circ$ . . . . .	20
Figure 9.	Wake Velocity Distribution at $\beta_1 = 48.0^\circ$ . . . . .	21
Figure 10.	Wake Velocity Comparision at $Y = 0.08c$ and $Y = 0.123c$ . . . . .	22
Figure 11.	Wake Velocity Comparision at $Y = 0.2c$ . . . . .	23
Figure 12.	Wake Velocity Comparision with LDV at $\beta_1 = 40.0^\circ$ . . . . .	24
Figure 13.	Wake Velocity Comparision with LDV at $\beta_1 = 46.0^\circ$ . . . . .	25
Figure 14.	Wake Turbulence Distribution at $\beta_1 = 40.0^\circ$ . . . . .	27
Figure 15.	Wake Turbulence Distribution at $\beta_1 = 46.0^\circ$ . . . . .	28
Figure 16.	Wake Turbulence Distribution at $\beta_1 = 48.0^\circ$ . . . . .	29
Figure 17.	Wake Turbulence Comparision at $Y = 0.08c$ and $Y = 0.123c$ . . . . .	30
Figure 18.	Wake Turbulence Comparision at $Y = 0.2c$ . . . . .	31
Figure 19.	Wake Turbulence Comparision with LDV at $\beta_1 = 40.0^\circ$ . . . . .	32
Figure 20.	Wake Turbulence Comparision with LDV at $\beta_1 = 46.0^\circ$ . . . . .	33

## LIST OF SYMBOLS

### Symbols:

$c$	Cord length of the blade
$M$	Mach number
$P$	Pressure
$R$	Gas constant
$R_e$	Reynolds number
$S$	Span of the blade
$V$	Velocity
$x,y$	Coordinates of the blade
$X$	Dimensionless velocity
$Y$	Axial displacement (downstream of the trailing edge)
$\beta$	Flow angle with respect to the direction normal to the line through the blade leading edges
$\gamma$	Stagger angle

### Subscripts:

0	Upstream of the guide vanes(plenum)
1	Upstream of the blade row(inlet)
2	Downstream of the blade row (outlet)
t	Total (stagnation)
wu	Upper wall
wl	Lower wall

## ACKNOWLEDGEMENT

I would like to express my appreciations to Dr. Raymond P. Shreeve, Director of Turbopropulsion Laboratory of Naval Postgraduate School, for his assistance in making this work a worthwhile learning experience. Also, thanks to Ted Best for his professional assistance.

Special thanks are due to my wife Gulay who gave her endless support while this study was going on.



# I. INTRODUCTION

Controlled diffusion blades have been developed in recent years for single and multistage compressor applications. These blades are designed analytically to be shock-free at transonic Mach numbers and to avoid suction surface boundary layer separation and ensure stable compressor operation over a wider range of inlet conditions. High efficiency and high loading capability using such blade shapes leads to reduced development costs and improved surge margin in aircraft engine compressors [Ref. 1].

A numerical optimization technique to design controlled diffusion (CD) compressor blading was developed by Nelson L. Sanger of the NASA Lewis Research Center and used to replace the double circular arc blading in the stator of a two-stage fan [Ref. 2]. The midspan of the redesigned blade row was subsequently tested in the subsonic cascade wind tunnel at the Turbopropulsion Laboratory, Naval Postgraduate School [Ref. 3]. The blade element performance was measured using calibrated pneumatic probe surveys, and surface pressure distributions and blade surface flow distributions were compared with the design and analysis expectations [Ref. 4].

In an attempt to resolve questions left in the earlier tests and to understand the loss behavior, John Dreon [Ref. 5] made wake measurements using a calibrated pneumatic probe. Dreon obtained data from  $0.12c$  to  $1.711c$  (where  $c$  is the chord length of the blade) downstream of the blade for air inlet angles of  $40.3$  and  $43.4$  degrees. The data showed that the near wake was quite asymmetric. The side of the wake from the pressure side of the blade showed a very steep velocity gradient while that from the suction side had a more gradual variation in velocity.

A more detailed study of the complete flow field through the CD blading was carried out recently by Elazar [Ref. 6] using a 2-component laser doppler velocimeter (LDV). As a part of that study, Elazar obtained wake data from  $0.04c$  to  $0.2c$  downstream of the blade for three inlet flow angles. The wake velocity and turbulence distributions were mapped downstream of the blade. The wake thickness was found to increase with increasing flow angles. In general, there was reasonable agreement with Dreon's data for the velocity magnitude, and some disagreement in the flow angle. However, no data were available with which to confirm the turbulence levels indicated by the LDV measurement technique.

Thus, the purpose of the present investigation was to retest the CD compressor stator blade in order to measure the wake downstream of the blade using a hot-wire system. The experiment was performed in the same subsonic cascade wind tunnel used by Elazar, with the same 20 CD blades installed in the test section. After preliminary work to interface and verify the hardware and the software of the hot-wire instrumentation, and to devise a probe system which would allow the hot-wire to be calibrated during the experiment, data were taken in the cascade at three stations from  $0.08c$  to  $0.200c$  downstream of the blade trailing edge for a total of three inlet flow angles from design to near stall condition.

In general, very good agreement was found between the single sensor hot-wire system and the two-component LDV measurements of both the mean velocity and the turbulence level at inlet angles of  $40.0$  and  $46.0$  degrees, despite the significant differences between the techniques. Data were also obtained at an inlet flow angle of  $\beta_i = 48.0^\circ$  for the first time.

In the present report, following a description of the wind tunnel facility and test section in Section 2, The IBM-PC/AT controlled TSI hot-wire system and its operation are described in Section 3. The experimental procedure and program of measurements are given in Section 4. The results are presented and discussed in Section 5 and the data are listed in tables in Appendix A. Finally, conclusions and recommendations are given in Section 6.



## II. TEST FACILITY

### A. CASCADE WIND TUNNEL

The subsonic cascade wind tunnel at the Turbopropulsion Laboratory of the Naval Postgraduate School was used for the present tests. A schematic diagram of the tunnel is given in Figure 1. The relevant features were outlined and a description of the flow in the tunnel was given by Sanger and Shreeve [Ref. 4: p. 46]. The test section instrumentation and physical dimensions are given in Figure 2. The CD blade coordinates are given in Table 1. The geometrical parameters of the cascade and the nominal test conditions are given in Tables 2 and 3 respectively.

The test facility was the same as that used by Dreon. The only differences compared to Dreon's work, were in the settings for the inlet flow angles, and in the dual-probe traverse and axial probe locations.

### B. PROBES AND TRAVERSE ARRANGEMENT

A dual-probe traverse arrangement was devised and installed to survey in the wake of the 7th cascade blade as shown in Figure 3. A TSI model 1210-T1.5 single sensor hot wire mounted in a Model 1150-18 probe support and Model 1152 right angle adapter were inserted into a modified United Sensor Corporation manual traverse unit such that the sensor was at the same station as the tip of a United Sensor Model PBC-24-G-22-KL Pitot-Static Probe. The manual (spanwise) traverse unit was mounted to a manual blade-to-blade traverse table, which was attached to the frame of the side wall. The axial location of the dual-probe arrangement was changed using aluminium blocks. The probe locations are shown in Figure 4.

### C. AUXILIARY INSTRUMENTATION

The plenum chamber total pressure was obtained using a pressure tube and the temperature was obtained with a thermocouple suspended into the plenum. A second pitot-static tube aligned with the inlet flow was used to obtain inlet total and static pressures. The pressures from the plenum and the two pitot-static probes were connected to a 10-tube water manometer referenced to atmosphere. Plenum and inlet flow conditions were recorded to obtain inlet velocity, Mach number and Reynold number. The calculation of the reference conditions is given in the Appendix B.

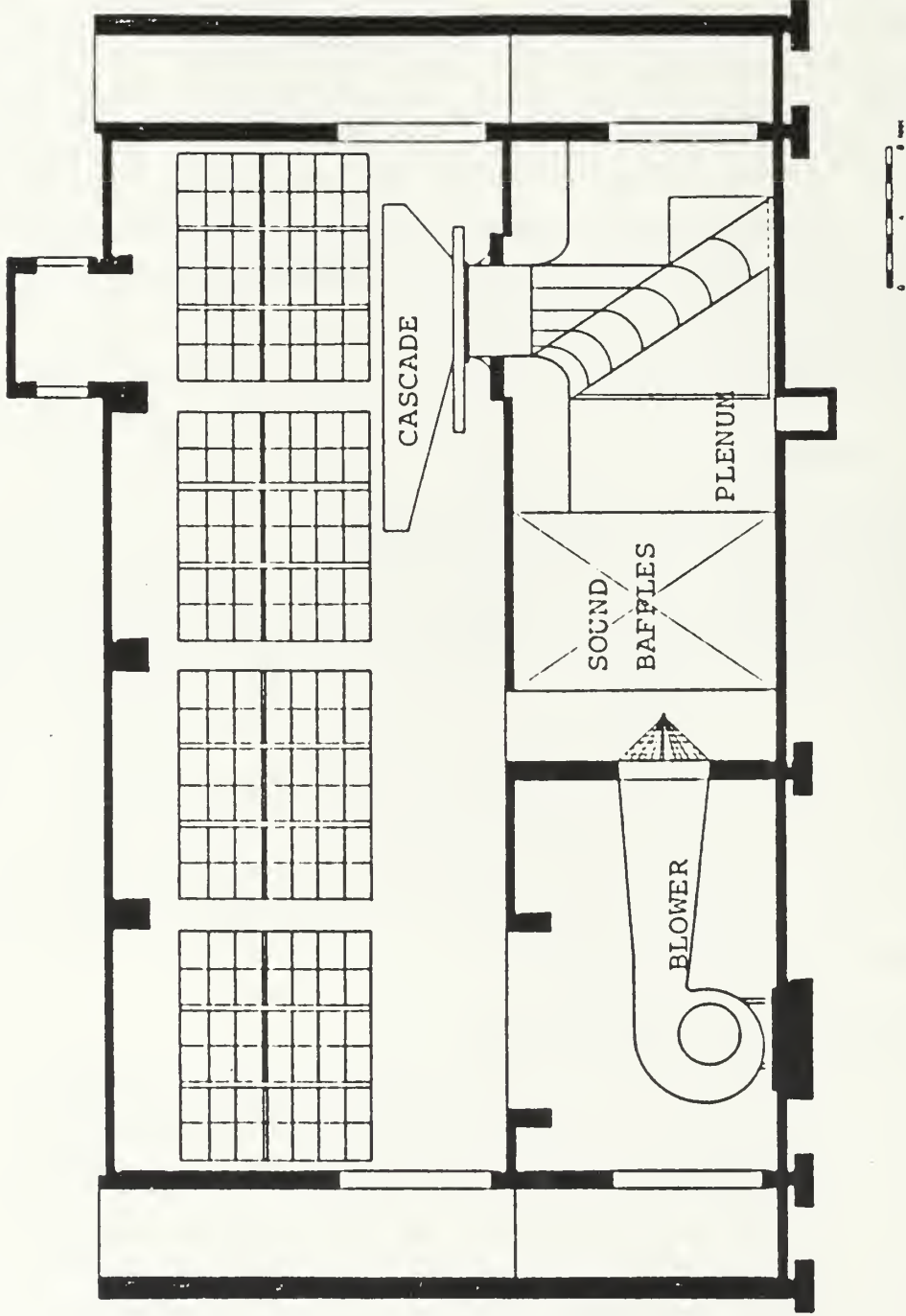


Figure 1. Cascade Wind Tunnel Schematic

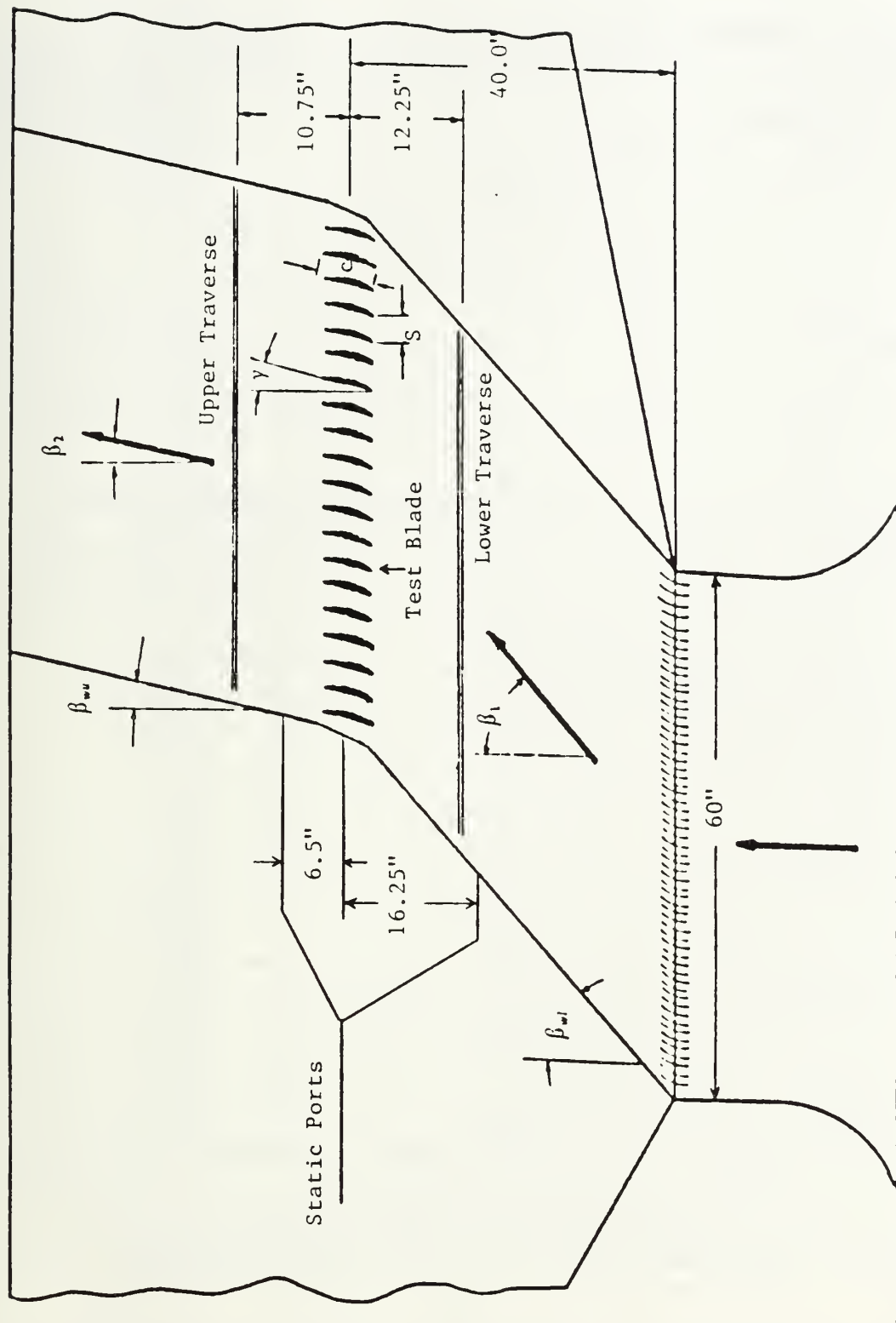
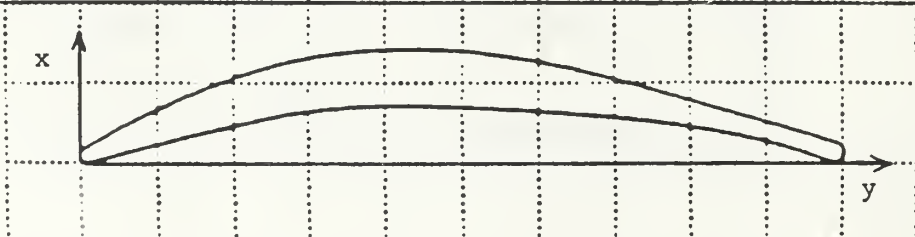


Figure 2. Cascade Test Section Instrumentation and Physical Dimensions.

Table 1. COORDINATES of the CD BLADE

x-coord.(in)	y-coord.(in)(pressure side)	y-coord.(in)(suction side)
0.000	0.045	0.045
0.022	-----	0.084
0.057	0.002	-----
0.222	0.044	0.196
0.444	0.101	0.307
0.666	0.155	0.403
0.888	0.207	0.488
1.110	0.255	0.561
1.332	0.299	0.621
1.554	0.330	0.663
1.776	0.350	0.691
1.998	0.359	0.705
2.220	0.359	0.708
2.442	0.352	0.701
2.664	0.342	0.681
2.886	0.331	0.650
3.108	0.317	0.610
3.330	0.301	0.563
3.552	0.281	0.510
3.774	0.257	0.453
3.996	0.227	0.393
4.218	0.191	0.332
4.440	0.146	0.270
4.662	0.089	0.208
4.882	0.019	0.145
4.925	0.004	-----
4.964	-----	0.122
5.010	0.062	0.062



**Table 2. GEOMETRICAL PARAMETERS of the CASCADE**

Number of Blades	20
Chord	5.01"
Blade Spacing	3.0"
Solidity	1.67
Thickness	7% Chord
Leading Edge Radius	0.045"
Trailing Edge Radius	0.062"
Setting Angle	$14.2 \pm 0.1^\circ$
Stagger Angle	$14.4 \pm 0.1^\circ$
Span	10.0"

**Table 3. NOMINAL TEST CONDITIONS**

$T_{t1}$	530 R°
$P_{t1}$	1.032 atm.
$P_2$	1.00 atm.
M	0.25
$R_c$	700,000



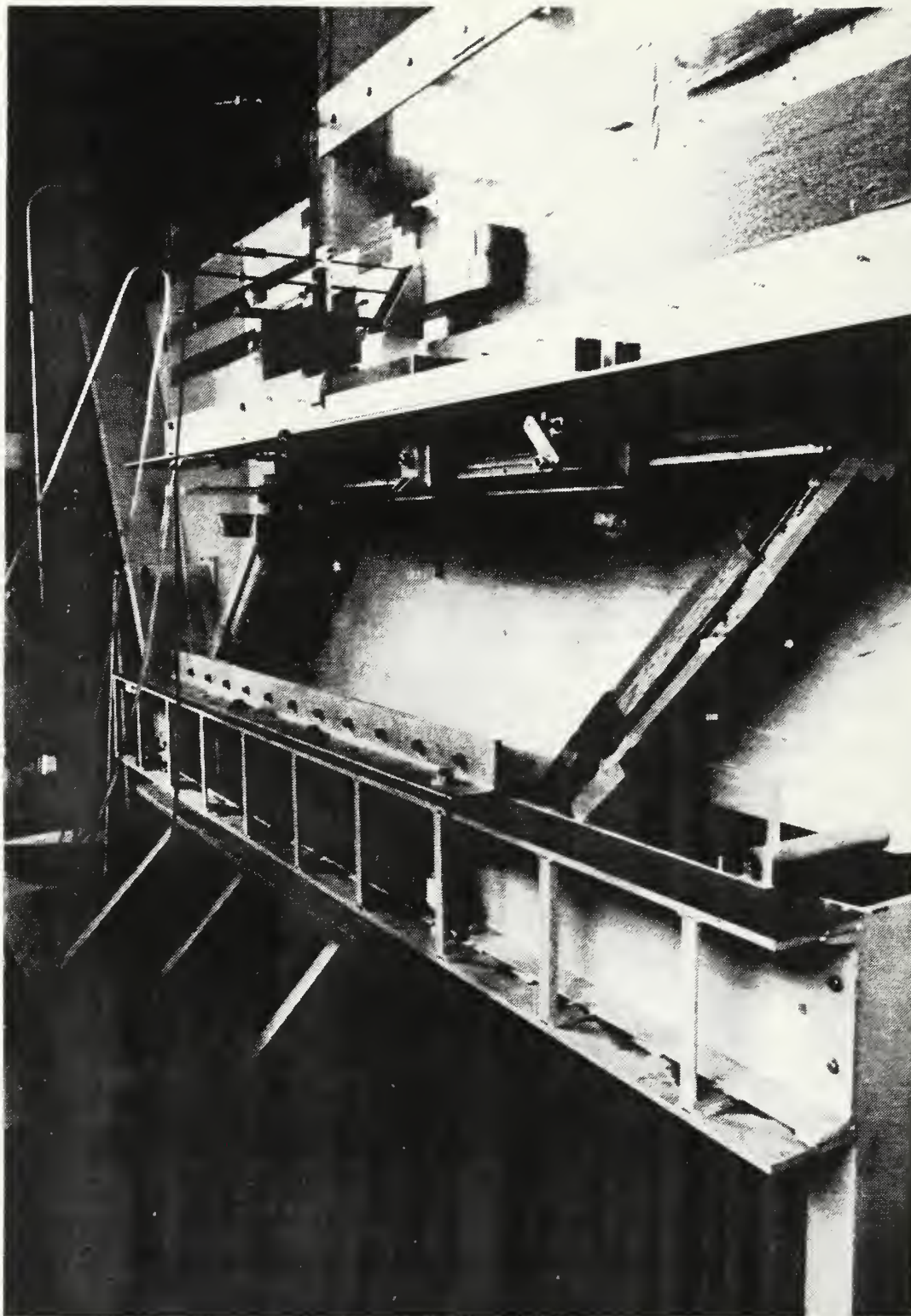
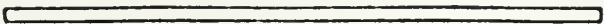
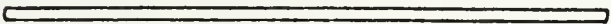
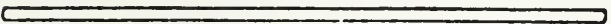
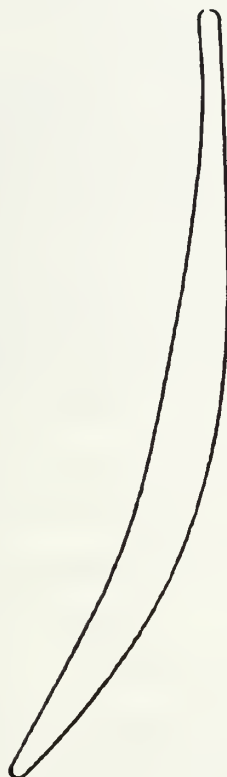


Figure 3. View of the Cascade Wind Tunnel and Dual-Probe Traverse Installation.



	Downstream of the blade trailing edge	
STATION #3		0.200c
STATION #2		0.123c
STATION #1		0.080c
	(not to scale)	



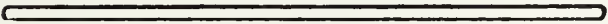
	Upstream of the blade leading edge	
	(not to scale)	
STATION #i		1.0c

Figure 4. Probe Survey Stations.

### III. HOT-WIRE SYSTEM

#### A. HARDWARE

The hot-wire system consisted, as shown in Figure 5., of the probe, the TSI IFA 100 Anemometer, TSI IFA 200 Digitizer and an IBM PC-AT. The computer system included 512K of memory, a 10MB hard disk and two 1.2MB floppy disks, a printer adapter card and a color graphics card, and a math co-processor. A TSI 6260 parallel interface card and a serial/parallel adapter were used to communicate with the IFA 100 and IFA 200.

#### B. SOFTWARE AND DATA ACQUISITION:

The TSI data analysis package (DAP) was used to obtain detailed fluid dynamic properties from the voltage output of a multi-element thermal anemometer system. One or two component data can be obtained depending on the probe used. The analog probe outputs from each anemometer channel are digitized and sent to the computer. The digitized data are converted to velocity using calibration information. At the same time the data are corrected for the effect of temperature on the velocity.

The IFA Thermal Anemometry Software Package is made up of six program packages ;

- Calibration Program
- Data Acquisition Program
- Statistical Analysis Program
- Spectrum Correlation Program
- Traverse Table Control Program
- Flow Field Plot Program.

The interrelation between the programs is illustrated in Figure 6.

##### 1. Calibration Program

This is a stand alone program in the IFA Thermal Anemometry Software Package. The program is used to calibrate single-, cross- and triple sensor probes. The voltage is fitted to a fourth order polynomial, the constants of which are used to produce "look-up tables". The look-up table for a particular probe is used with data taken with the acquisition program, to find the velocity corresponding to the deconditioned, temperature-corrected, digitized voltage.

Four methods may be used to calibrate; namely,

- a. using data taken with the IFA 100 and 200 and a pressure transducer.

- b. using data taken with the IFA 100 and 200 and manually entering differential pressure.
- c. using data taken with the IFA 100 and 200 and manually entering velocity,
- d. by manually entering bridge voltage and pressure directly. In this case no data are acquired from the IFA 100 via DMA.

## **2. Data Acquisition Program**

This program is designed to acquire data with 1, 2 and 3 sensor hot-wire configurations. It allows control of the anemometer and digitizer systems. It can take data up to 16 channels and store them in raw data files. The communication between the computer and the IFA 100 or IFA 200 can also be verified in this program.

## **3. Statistical Analysis Program**

This program generates the velocity data and the statistics from the raw data files created by the Data Acquisition Program. The look-up tables are used when converting the raw voltage into an effective velocity. During the statistical data processing, no additional parameters are entered to build the velocity data and statistics. All the parameters required by the program are set in the Data Acquisition Program and saved in the header of the raw data file. The Statistical Analysis Program constructs the velocity data and statistics for all probes that are defined when data are collected. It combines single-, cross- and triple-wire probes signals when collecting data. The program then constructs the velocity data and statistics for all of them at one time. Finally the program saves the data in the velocity and statistics files.

## **4. Spectrum Correlation Program**

This program builds the signal spectrum, the signal auto-correlation and the two-signal correlation functions. It uses the velocity data produced by the statistics analysis program. The spectra and correlations are built using a Fast Fourier Transform (FFT) algorithm for spectra. The data are transformed to the frequency domain to be averaged and smoothed with the Hanning window. For correlations, the data are transformed to the frequency domain, multiplied by the conjugates of one another and transformed back to the time domain for averaging. Both processes use the segmentation method to transform the data.

This program allows the construction of the requested spectrum or correlation using segmentation and the FFT. These can be displayed on the screen, plotted or printed out as tables. The data can be saved for future processing.

## **5. Traverse Table Control Program**

This program allows independent control of the movement of the Traverse Table. It also constructs an automatic traversing matrix that can be used as a list of coordinate positions. The Data Acquisition Program will use this matrix to automatically collect data along a pre-determined coordinate path. This program can be used with a TSI computer-controlled traverse table. Alternatively, the position of the probe can be entered manually, to be recorded with the corresponding data. This was done in the present study.

## **6. Flow Field Plot program**

This program is designed to plot statistical values such as mean velocity, RMS, skewness coefficients, flatness coefficients, and correlation coefficients vs the probe position. The inputs to the program are the raw data files and the analysis files generated by the Data Acquisition Program and Statistics Analysis Program. Multiple data files can be used to plot any statistical parameter as a function of position.

The program offers four important functions:

- The plot-file can read up to 30 family filenames; each family can have up to 99 data files.

- The plot can generate up to 400 statistical positions.

- The data used in the plot can be printed on a printer.

- The plots may be non-dimensionalized, automatically scaled, or manually scaled.

More detailed information is given in [Ref. 7].

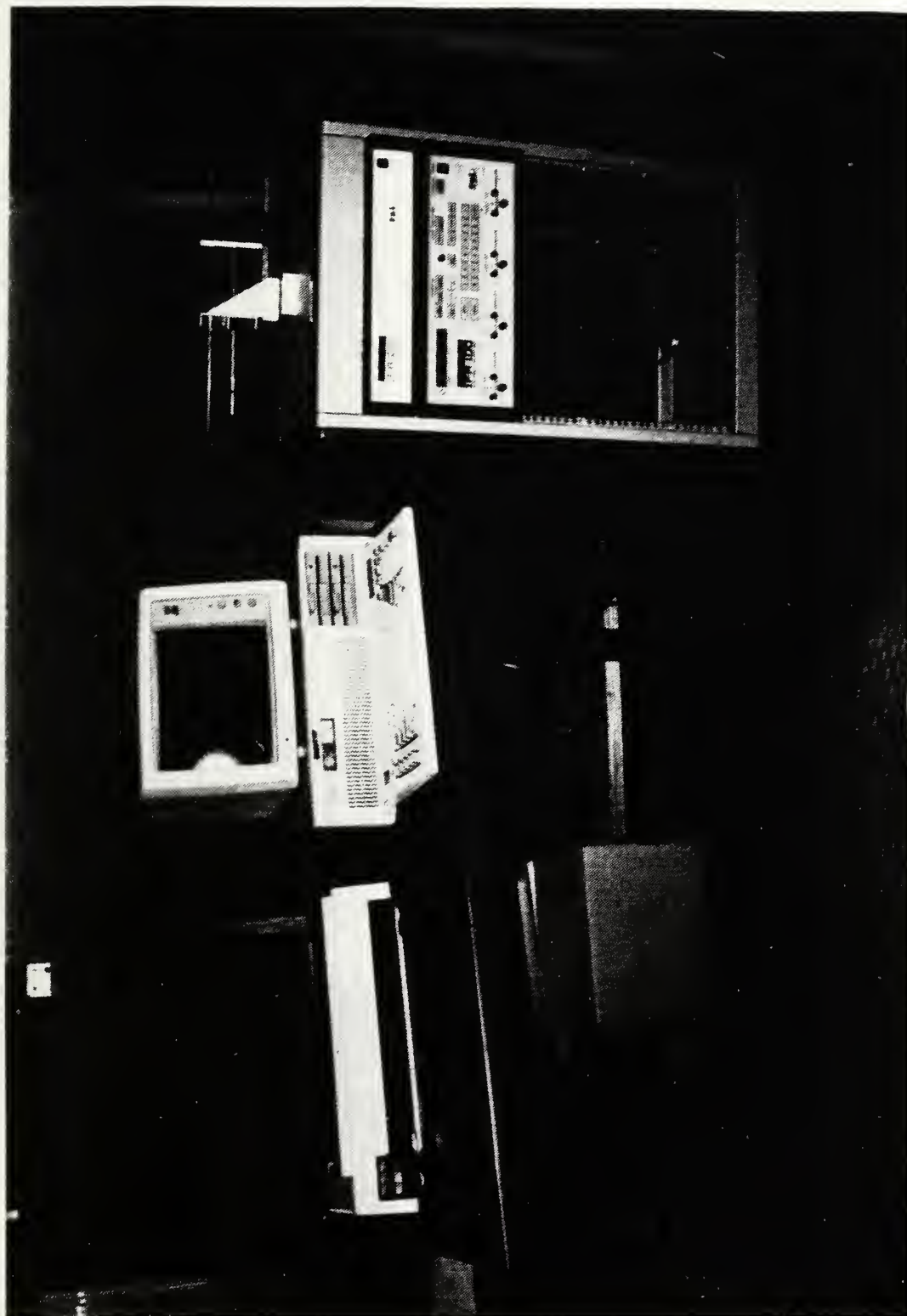


Figure 5. Hot-Wire System Hardware

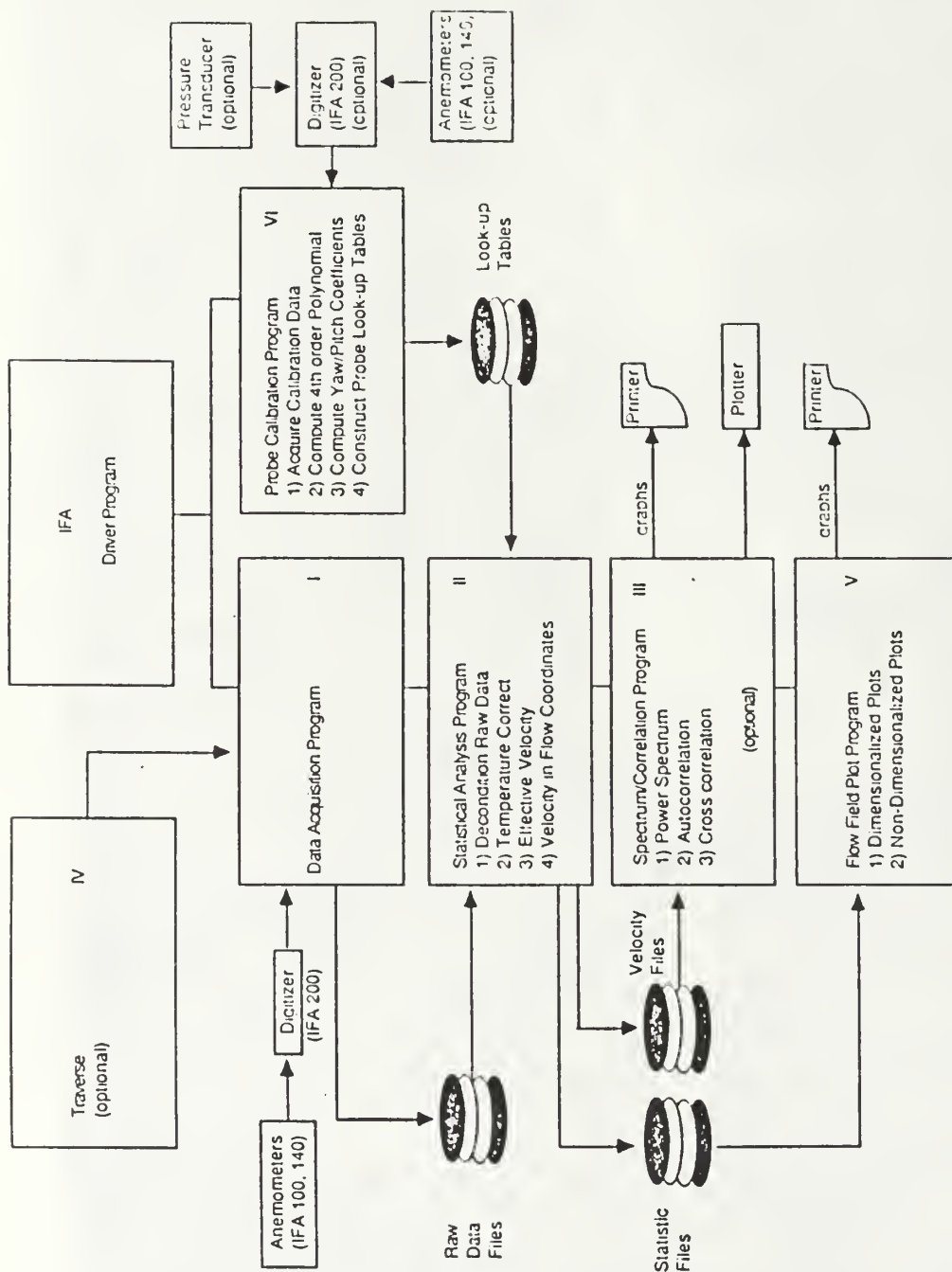


Figure 6. Software Flow Chart



## **IV. EXPERIMENTAL PROCEDURE**

### **A. TEST SECTION SET UP AND ADJUSTMENTS.**

Prior to measurements of each inlet flow angle, the front plexiglas wall of the wind tunnel was removed and the inlet wall angle and IGV's were set. The wall was replaced, the tunnel was started and the tailboard angles were adjusted to get a uniform outlet static pressure distribution. The absence of leaks was checked very carefully. Then the experiment was performed for the current inlet condition.

### **B. SURVEY PROCEDURE**

#### **1. Probe Calibration**

Prior to the experiment, the IFA 100 Flow Analyzer and IFA 200 Digitizer were made ready to take data. First, a shorting probe was inserted into the probe holder and the probe cable resistance was measured. The value was entered into the IFA 100 memory. Then the shorting probe was removed and the hot-wire was inserted into the probe holder. The probe resistance was measured and recorded into the IFA 100 memory. Related to the cable resistance and the cold resistance, the operating resistance was obtained and entered into the memory. (The software is designed to accept those values and to enter them into the program for future use. The resistance values are assigned to the particular probe serial number and channel number to which it is connected).

The signal conditioner was adjusted to span the minimum and maximum wire voltages to be recorded during the measurements. These voltages correspond to minimum and maximum expected flow velocities. While acquiring velocity data, the changes of the supply temperature were recorded and entered into the program to facilitate corrections. A complete description of the calibration procedure is given in [Ref. 7: p. 45].

The probe calibration was carried out immediately prior to measurements with the hot-wire installed in the dual-probe traverse mechanism in the cascade wind tunnel. The probes were traversed to a position outside of the blade wake where the flow was uniform. The hot-wire sensor and the pitot-static tube total pressure hole were at the same axial station. The span-wise traverse was adjusted so that the two probes were also equidistant from mid-span. The first point in the calibration was with the tunnel off. Then, the tunnel was started, and for a number of wind tunnel speeds up to the desired operating speed, calibration data were recorded. At each speed, the hot-wire output was

sampled and the corresponding pitot-static pressure differential was entered as requested. The program then fitted these data with a fourth order polynomial of velocity vs. voltage and calculated the five constants. The five constants were saved in a file, referred to as a "Look-up table" and also stored in every subsequent raw data file containing measurements.

## 2. Surveys

### a. Upstream Probe Survey

A preliminary survey was made with the upstream pitot-static probe approximately 4.75 inches upstream of the test blade. When it was verified that the velocity did not vary in the blade-to-blade direction, the probe was fixed at a station one blade passage away from the test blade to avoid disturbing the flow around the test blade. The probe was aligned carefully to inlet flow direction.

### b. Downstream Probe Survey

The hot-wire in the dual-probe system was located at midspan in midpassage and traversed in the blade-to-blade direction through the wake of the test blade. Data were recorded across one blade spacing for a total of 33 points. The increments were 0.1-0.2 inches outside and 0.05 inches inside the wake.

## C. PROGRAM OF MEASUREMENTS

The data were taken at three axial stations for a total of three inlet flow angles from on design to near stall conditions. The program of measurements is given in Table 4.

Table 4. PROGRAM of MEASUREMENTS

RUN	DATA SET	$\beta_1$	$y/c = 0.080$	$y/c = 0.123$	$y/c = 0.200$
1	1	40.0°	X		
	2	40.0°		X	
	3	40.0°			X
2	1	46.0°	X		
	2	46.0°		X	
	3	46.0°			X
3	1	48.0°	X		
	2	48.0°		X	
	3	48.0°			X

## V. RESULTS AND DISCUSSION

### A. WAKE VELOCITY DISTRIBUTIONS

The plots of the downstream wake surveys are given in Figures 7-9 for inlet flow angles  $\beta_1 = 40.0^\circ$ ,  $\beta_1 = 46.0^\circ$  and  $\beta_1 = 48.0^\circ$  respectively. The velocity shown on the plots was made non-dimensional with respect to inlet flow velocity.

In general, the wake shape downstream of the blading was qualitatively as expected following Dreon [Ref. 5: p. 38]. The pressure side of the wake had a very steep velocity gradient while the suction side had a more gradual velocity gradient.

The magnitude of the wake velocity changed depending on inlet flow angle and the axial displacement. For design inlet conditions, ( $\beta_1 = 40.0^\circ$ ) the wake was nearly symmetric at the three axial stations. As can be seen from Figure 7, the freestream velocity decreased from the first downstream location to far downstream while the minimum velocity in the wake increased. The freestream velocity was about 86% of the inlet flow velocity and the minimum was about 18% of the inlet velocity at  $Y=0.08c$ . The free stream velocity decreased to 84% and the minimum increased to 40% of the inlet flow velocity at  $Y=0.2c$ .

At higher inlet flow angle,  $\beta_1 = 46.0^\circ$ , the wake velocity distribution at the suction side of the blade became thicker with a reduced velocity gradient while the pressure side kept nearly the same shape as for the design condition. The change in the magnitudes of the velocities can be seen in Figure 8. The freestream velocity was about 80% of the inlet flow velocity. The minimum velocity was about 11% at  $Y=0.08c$ , 17% at  $Y=0.123c$  and 26% at  $Y=0.2c$  with respect to inlet velocity.

At  $\beta_1 = 48.0^\circ$ , the wake was even wider. However, the freestream velocity outside wake was about 86% of the inlet velocity at  $Y=0.08c$ , 85% at  $Y=0.123c$  and  $0.2c$  which was very similar to the design conditions. But the minimum velocity was about 13% of the inlet velocity at  $Y=0.08c$ , 18% at  $Y=0.123c$  and 24% at  $Y=0.2c$ , which were lower than the minimum velocities at design conditions.

The wake velocities at the three inlet angles are compared in Figures 10 and 11. It is noted that before the measurements were made, flow separation was expected to occur near the trailing edge of the blade at  $\beta_1 = 48.0^\circ$ . However, in an examination using tufts, no indications of separation or on-set of stall were found. Thus, the three wakes

shown in Figures 10 and 11 were generated from progressively thicker, but attached, boundary layers leaving the trailing edge of the blade.

The data obtained with the hot-wire system are shown for comparison with data obtained using the LDV [Ref. 6: p. 135] in Figures 12 and 13. Very good agreement was found at both  $\beta_1 = 40.0^\circ$  and  $\beta_1 = 46.0^\circ$ , at  $Y = 0.123c$ . No LDV data were taken at  $\beta_1 = 48.0^\circ$ .

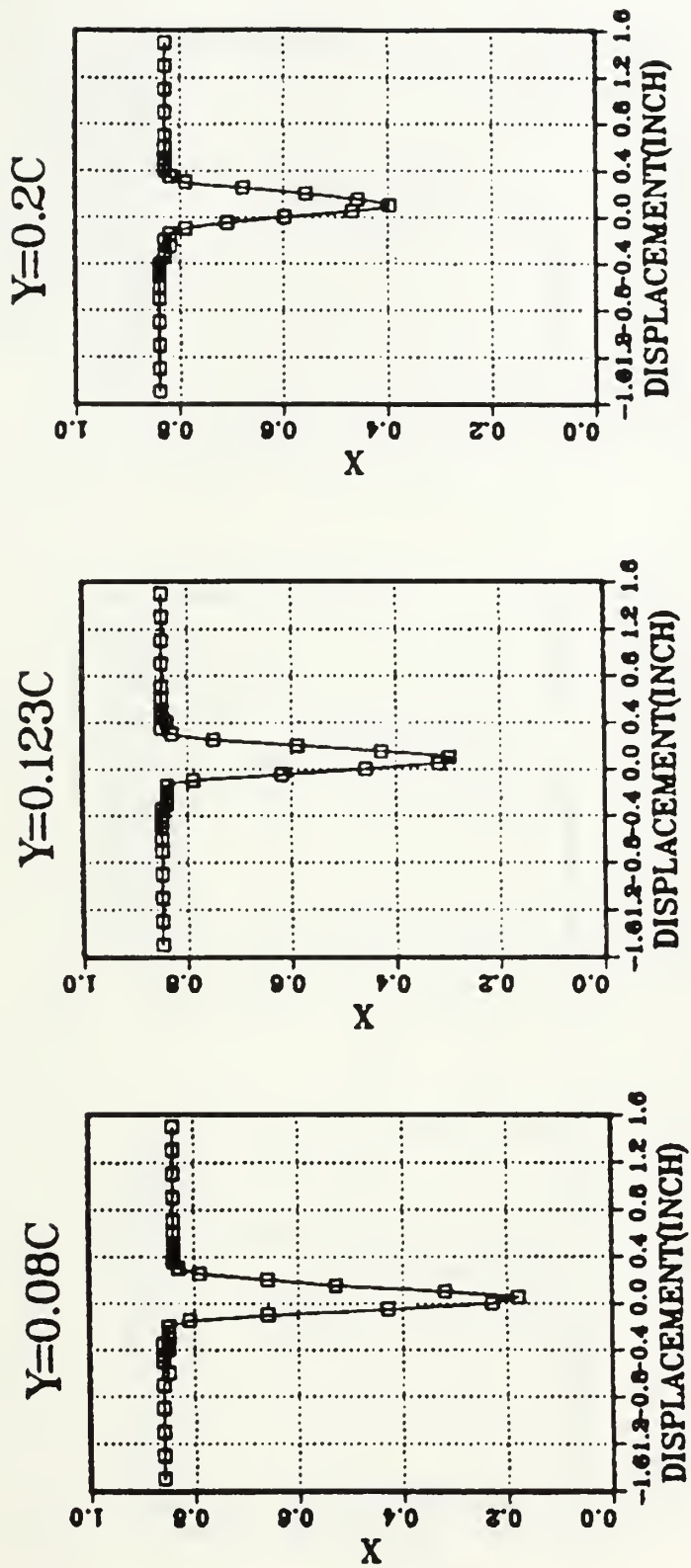


Figure 7. Wake Velocity Distribution at  $\beta_1 = 40.0^\circ$

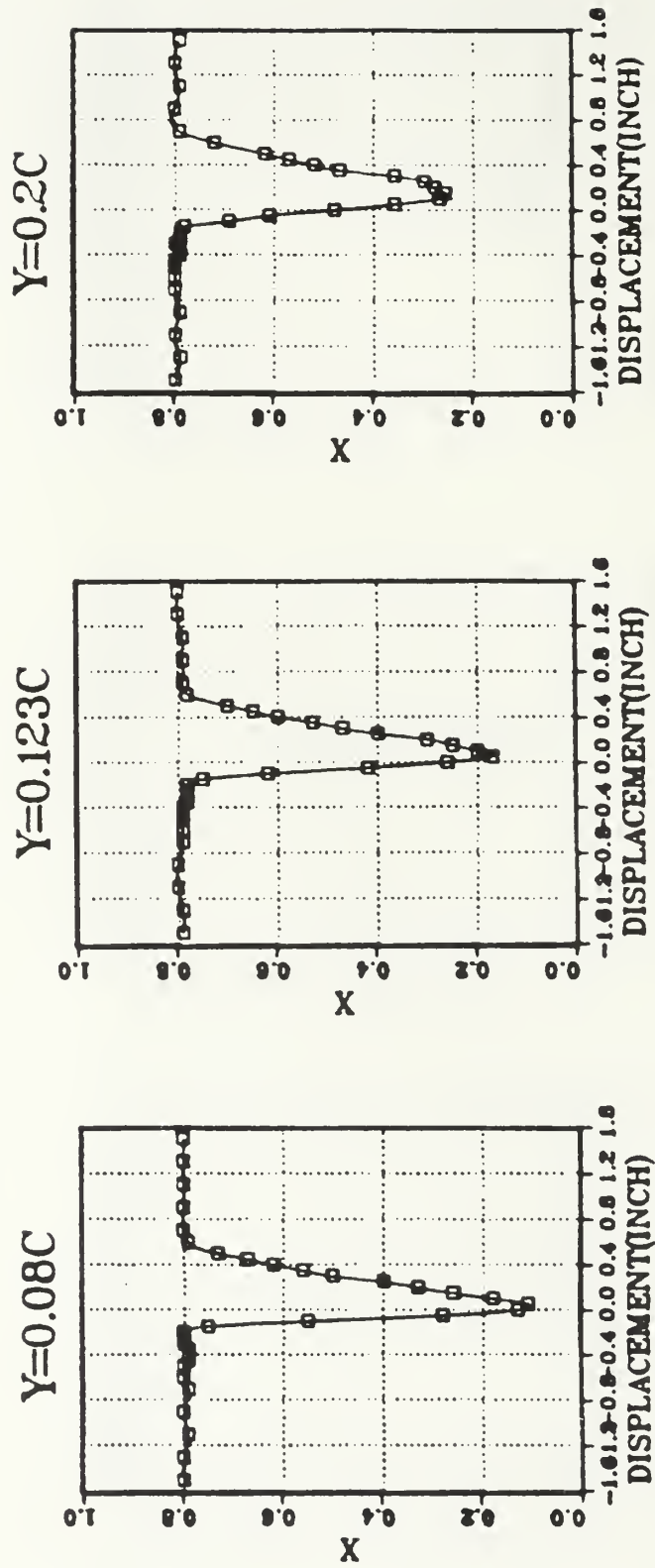


Figure 8. Wake Velocity Distribution at  $\beta_1 = 46.0^\circ$



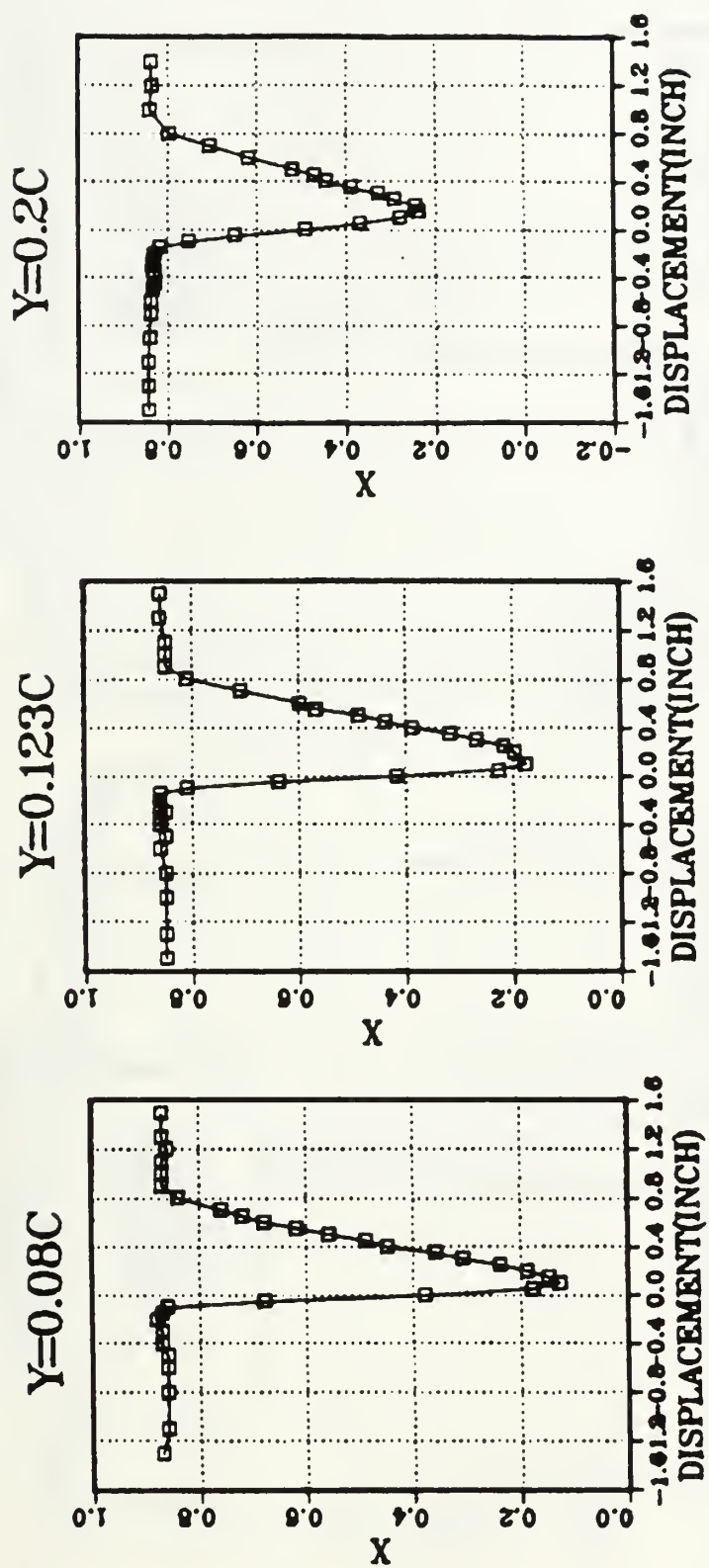
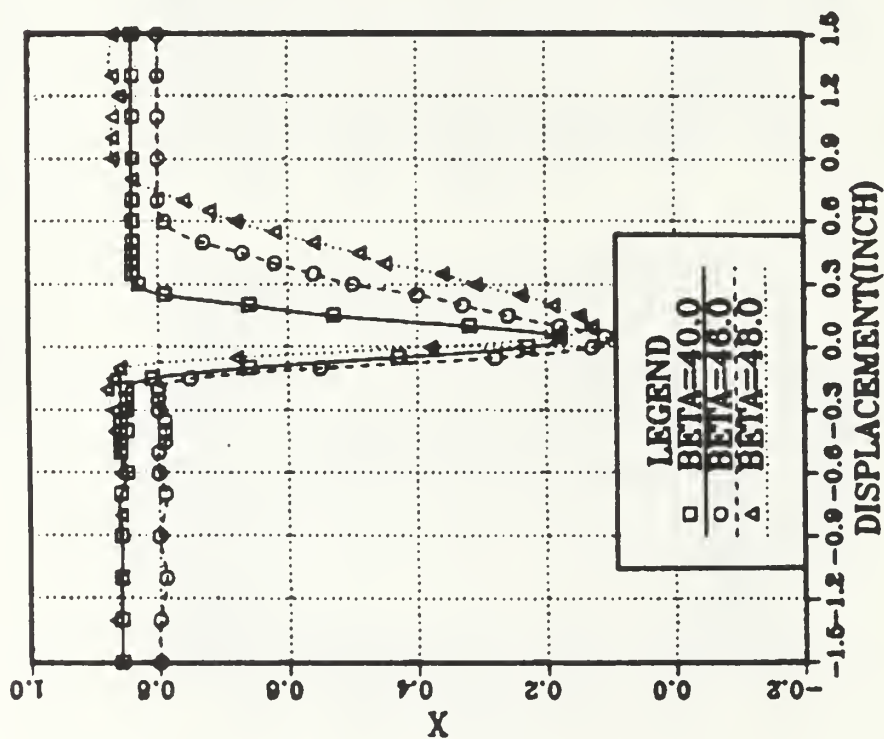


Figure 9. Wake Velocity Distribution at  $\beta_1 = 48.0^\circ$



$Y=0.08C$



$Y=0.123C$

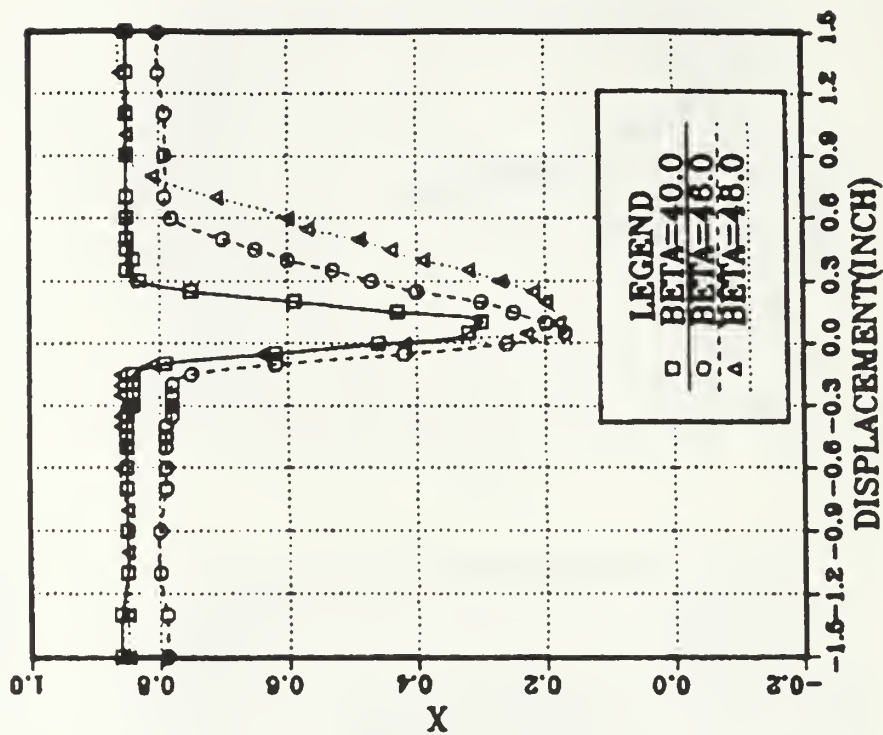


Figure 10. Wake Velocity Comparison at  $Y = 0.08c$  and  $Y = 0.123c$

$Y=0.2c$

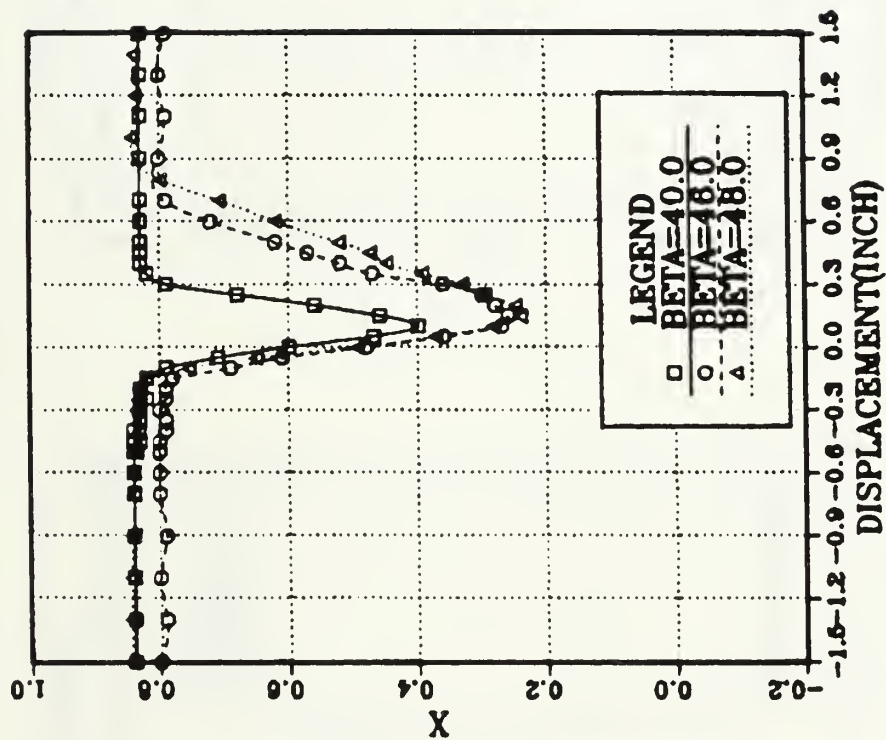
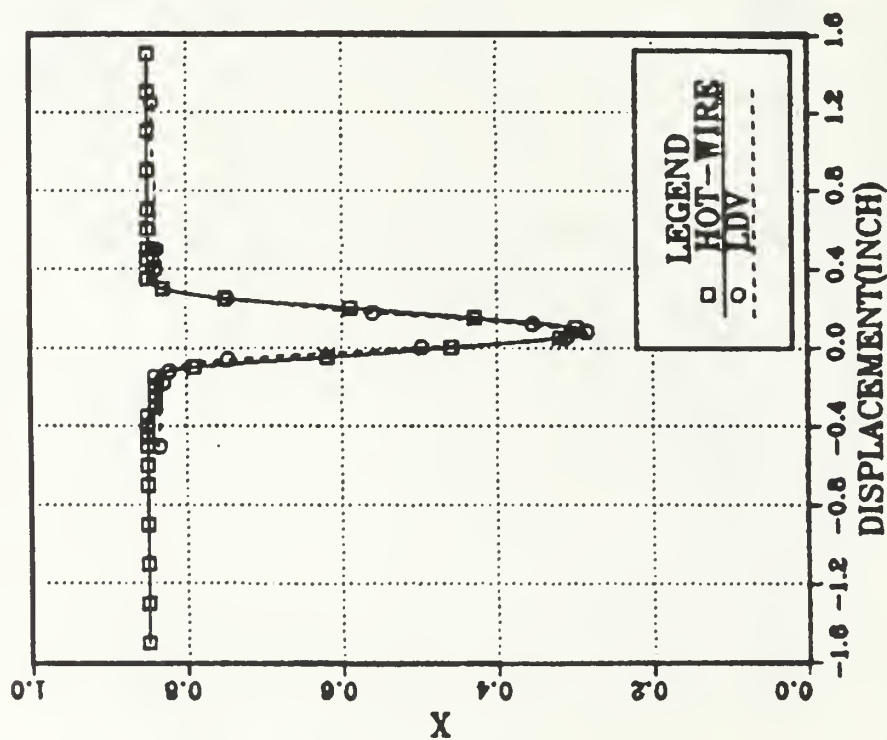


Figure 11. Wake Velocity Comparison at  $Y = 0.2c$

BETA=40.0 DEG. Y=0.123C



BETA=40.0 DEG. Y=0.2C

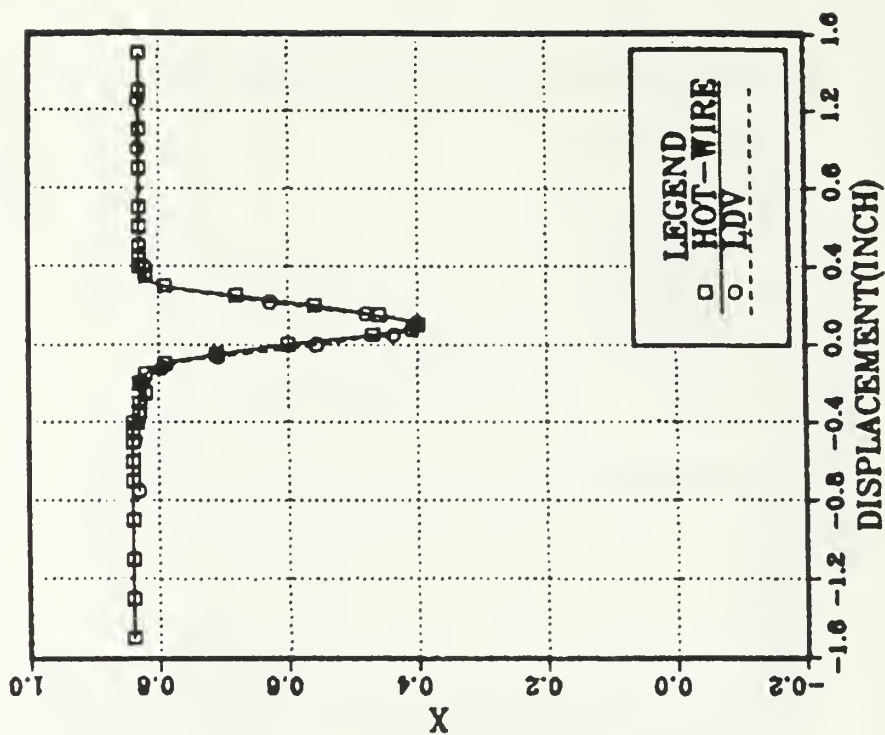
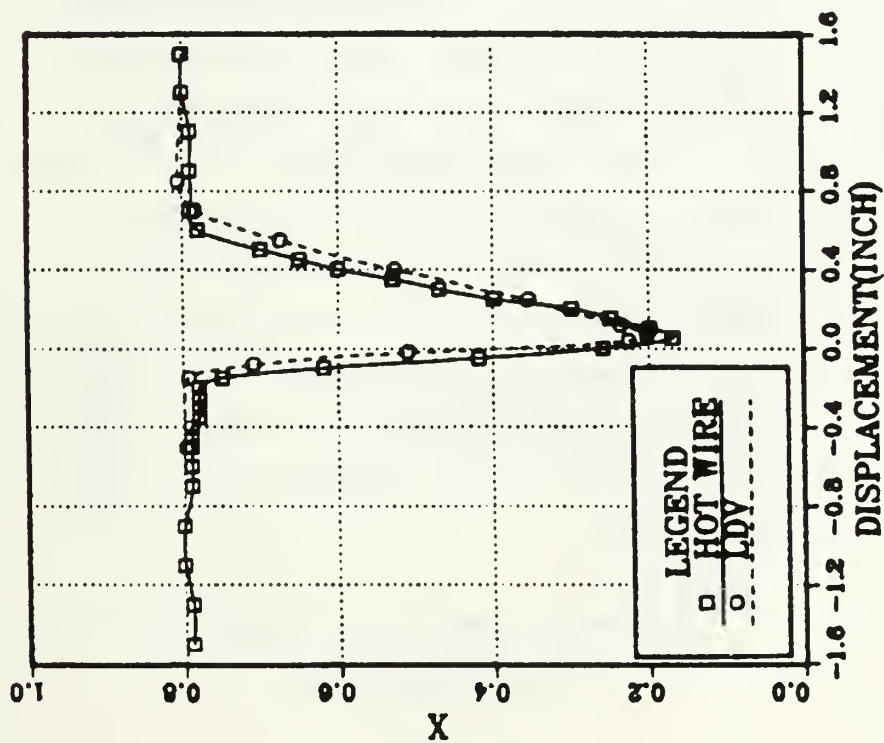


Figure 12. Wake Velocity Comparison with LDV at  $\beta_1 = 40.0^\circ$

BETA=46.0 DEG. Y=0.123C



BETA=46.0 DEG. Y=0.2C

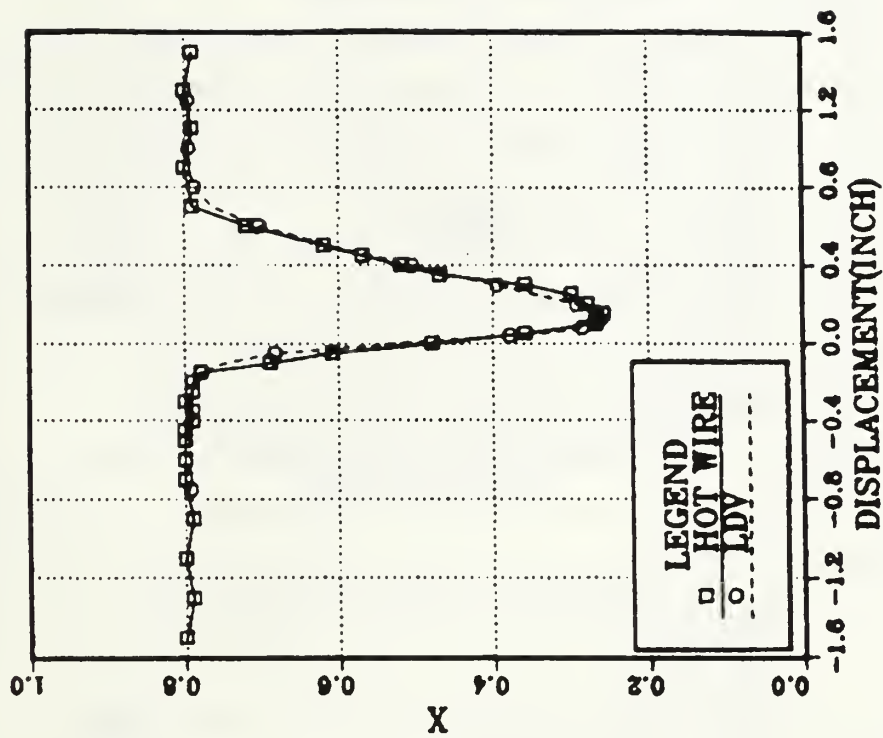


Figure 13. Wake Velocity Comparison with LDV at  $\beta_1 = 46.0^\circ$

## B. TURBULENCE INTENSITY DISTRIBUTIONS

Turbulence intensity measurements are shown in Figures 14-16. The comparisons at the three stations for the three inlet flow angles are given in Figures 17 and 18. Comparisons with LDV measurements at  $\beta_1 = 40.0^\circ$  and  $\beta_1 = 46.0^\circ$  are shown in Figures 19 and 20, respectively.

For the design condition, ( $\beta_1 = 40.0^\circ$ ), the pressure side of the wake had a peak turbulence level higher than the peak value on the suction side of the wake. The maximum values of about 10% were almost the same at  $Y = 0.08c$  and  $Y = 0.123c$ . The maximum declined to about 9% far downstream of the blade.

At the higher inlet flow angle of  $\beta_1 = 46.0^\circ$ , the peak values of the turbulence were on the suction side of the wake, in contrast to design conditions. The thickness of the turbulent region was wider than at the design condition, consistent with the velocity distribution at this inlet angle. The peak turbulence values were about 11% at all axial stations.

Close to the expected stall condition, at  $\beta_1 = 48.0^\circ$ , the turbulent layer was much thicker and the magnitude of the turbulence intensity was larger than at the other two inlet flow angles. There were also three peak values in the distribution, rather than two. The highest value was about 13% towards the suction side of the midpoint of the wake, the second was at the suction side of the wake with a magnitude of about 12%, the third was on the pressure side of the wake, with a magnitude of about 11%.

Comparisons with LDV data are shown in Figures 19 and 20. They were seen to agree very well except near the center of the wake. Significant differences can be seen in the plots. There are at least two possible explanations for these differences. The first is the fundamental difference in the measurements of the systems. The LDV takes two components of the turbulence and averages them, while the hot wire measures a single component. The contributions of the two velocity components need not necessarily be the same. The second possibility is that the particles measured by the LDV do not follow the flow perfectly in these regions.

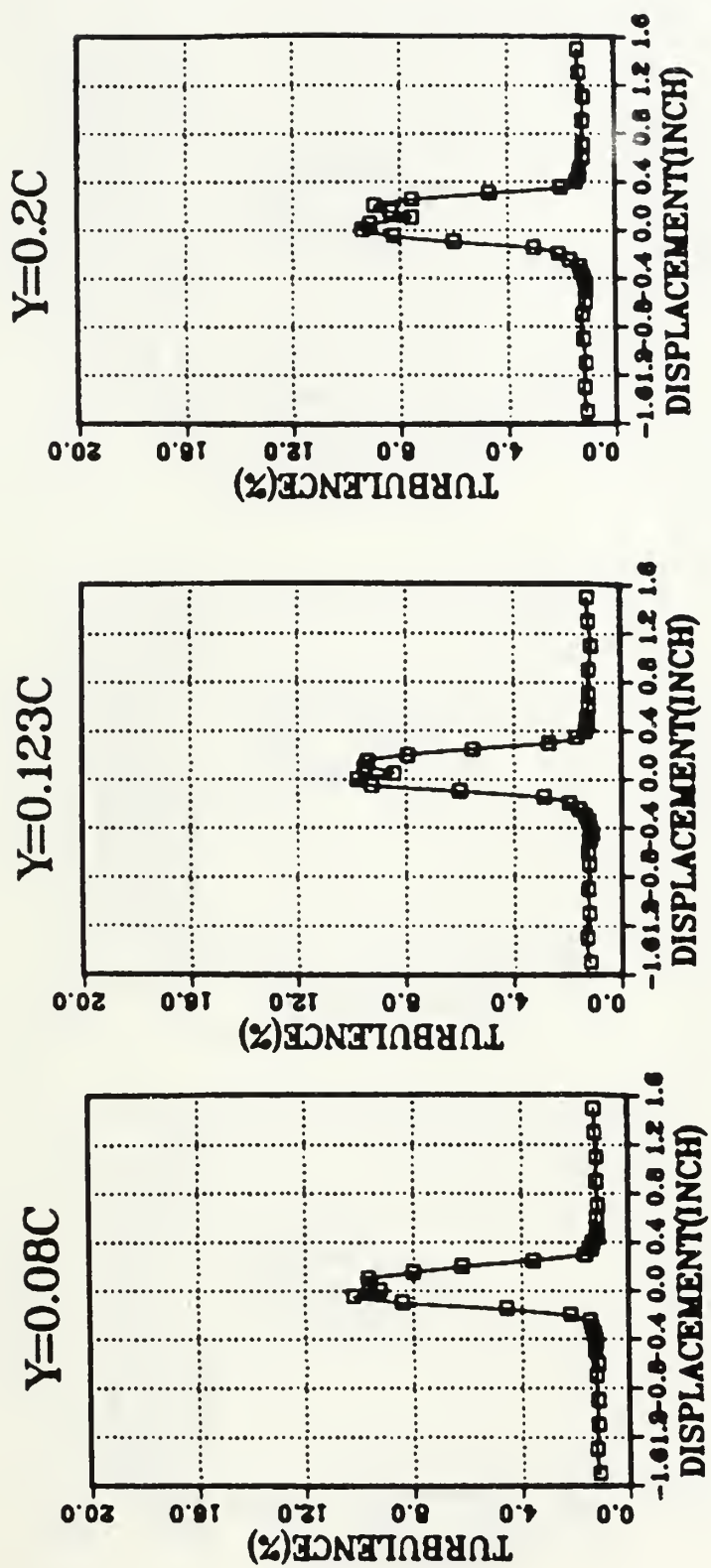


Figure 14. Wake Turbulence Distribution at  $\beta_1 = 40.0^\circ$



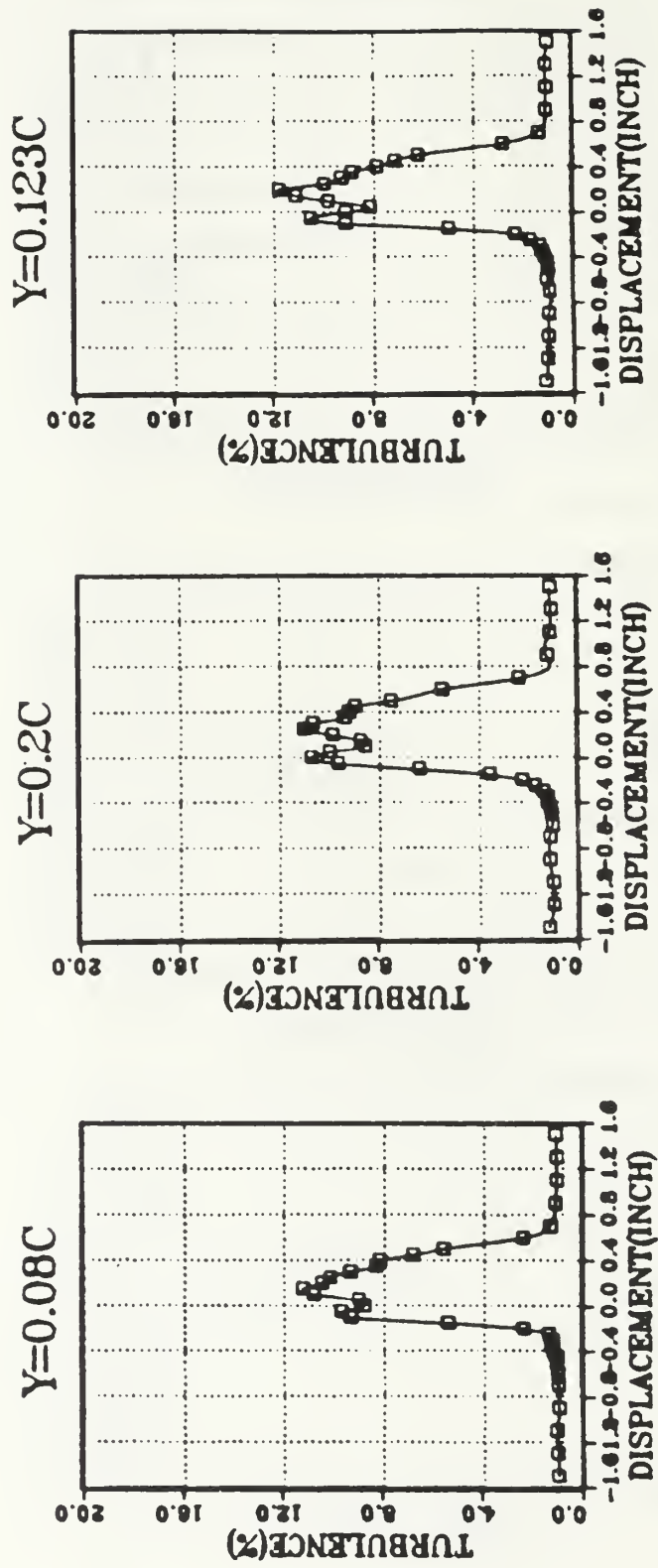


Figure 15. Wake Turbulence Distribution at  $\beta_1 = 46.0^\circ$



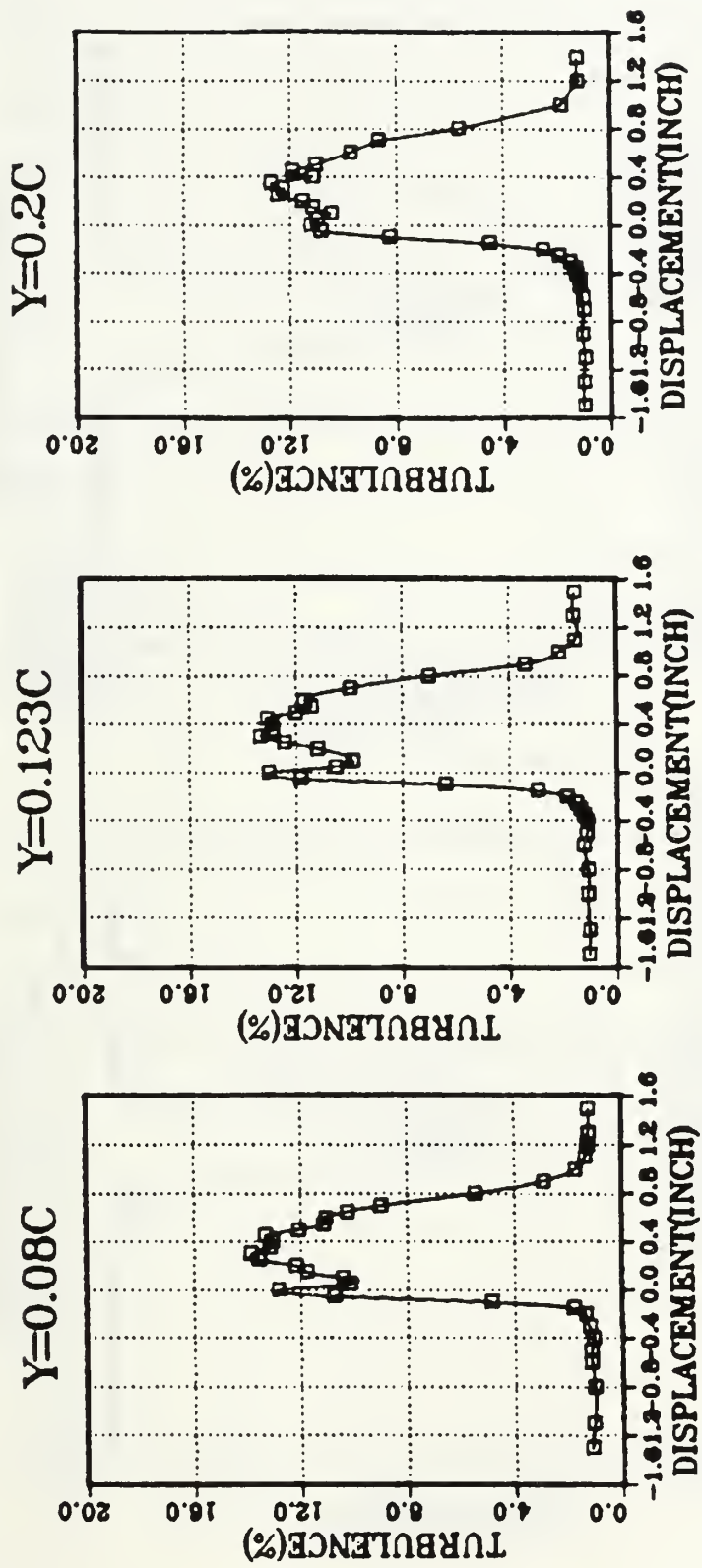
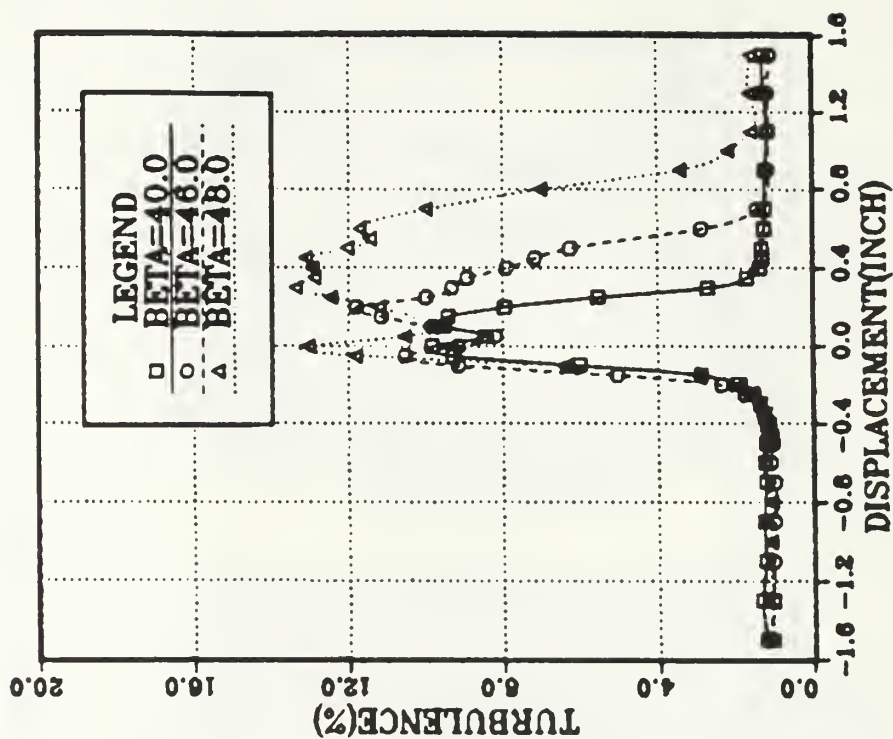


Figure 16. Wake Turbulence Distribution at  $\beta_1 = 48.0^\circ$

Y=0.123C



Y=0.08C

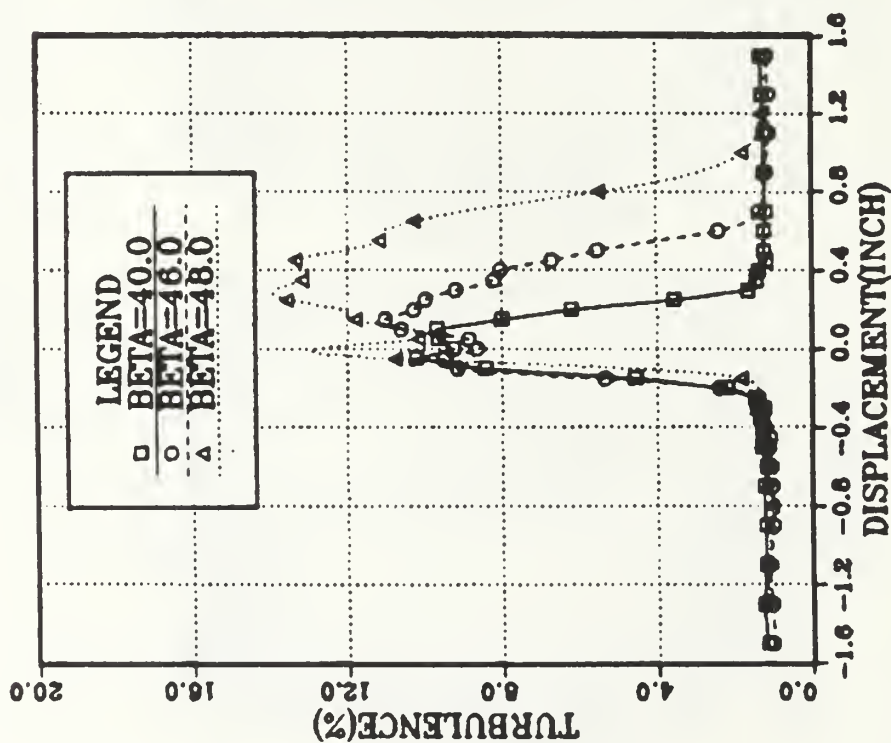


Figure 17. Wake Turbulence Comparison at  $Y = 0.08c$  and  $Y = 0.123c$

Y=0.2C

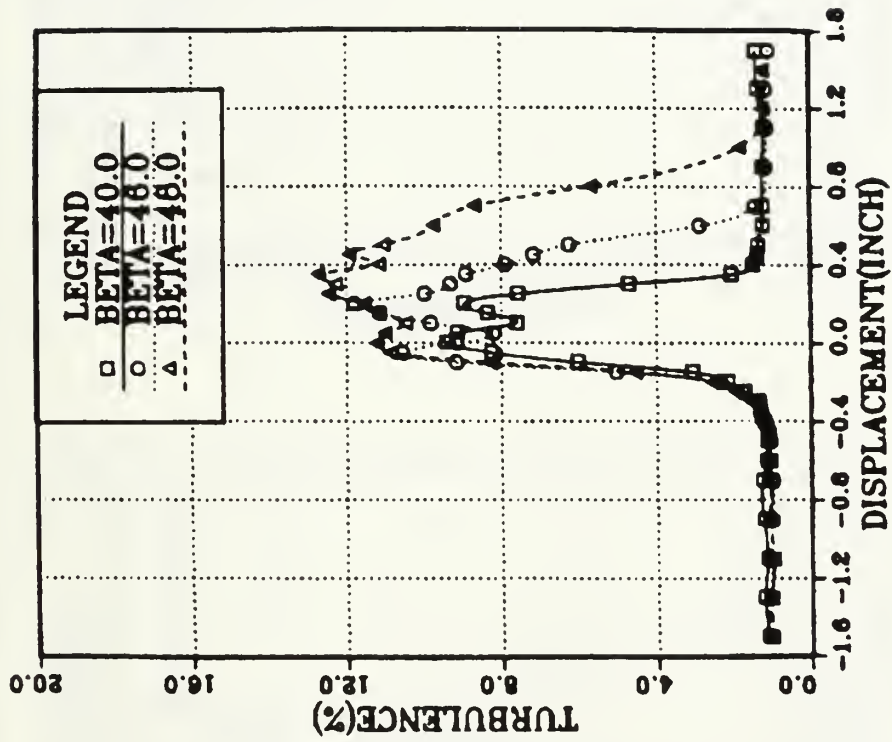
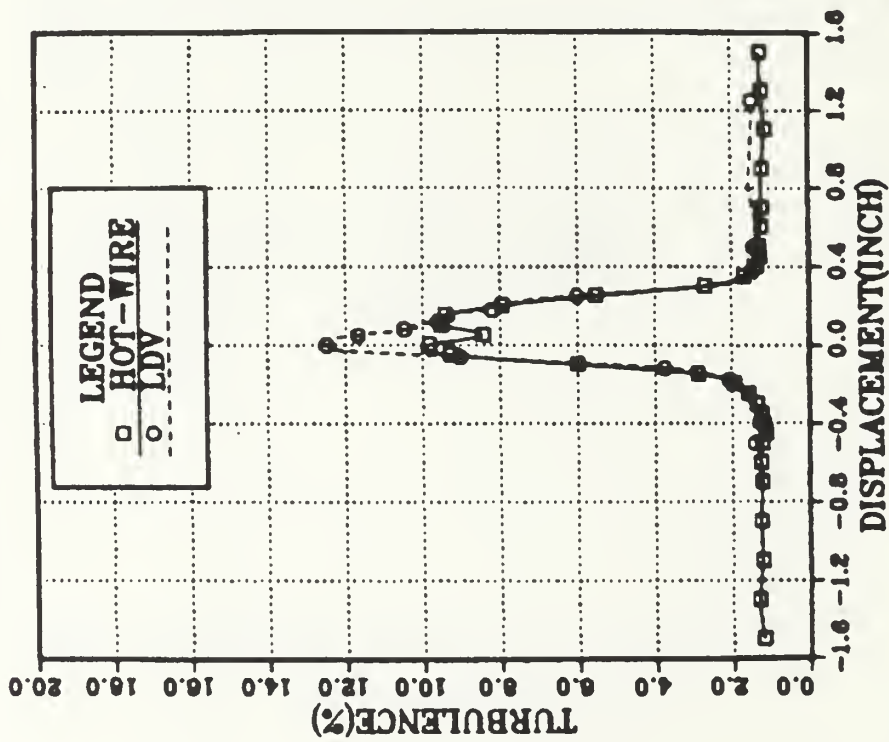


Figure 18. Wake Turbulence Comparison at  $Y = 0.2c$

BETA=40.0 DEG. Y=0.123C



BETA=40.0 DEG. Y=0.2C

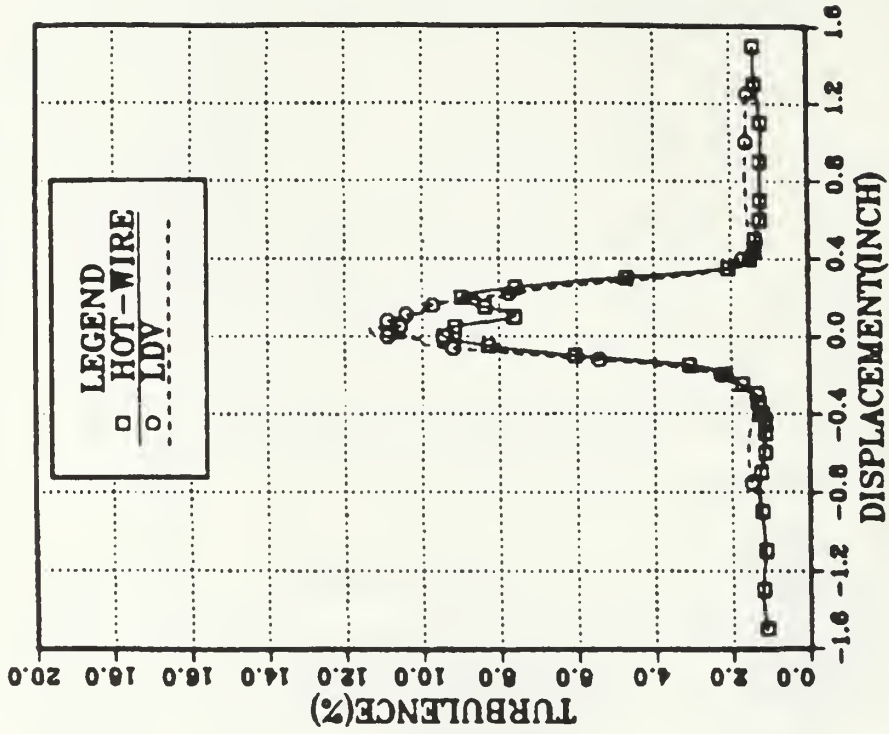
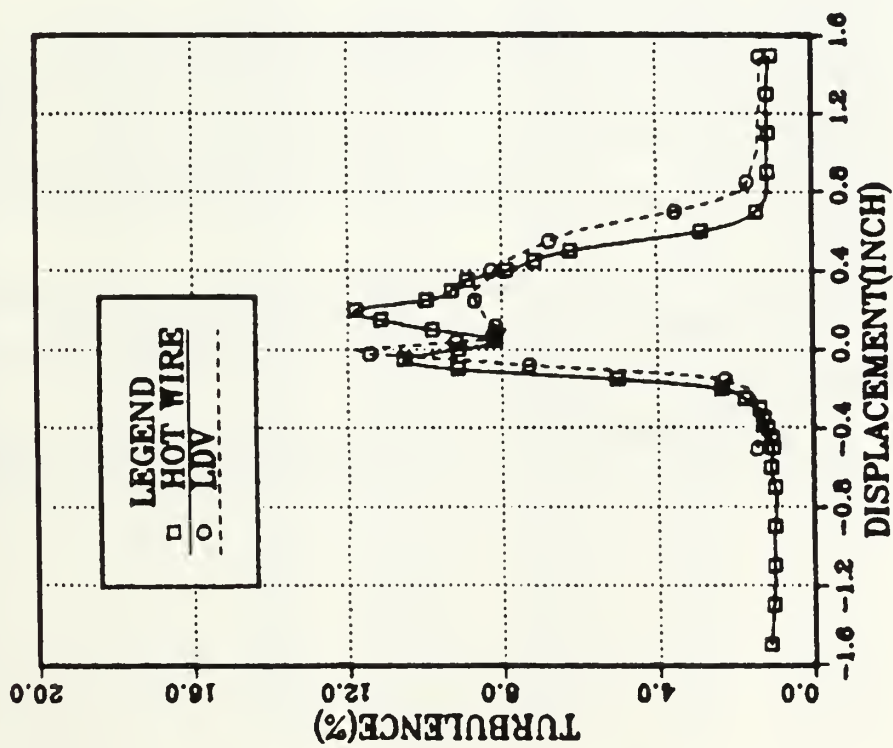


Figure 19. Wake Turbulence Comparison with LDV at  $\beta_1 = 40.0^\circ$

BETA=46.0 DEG. Y=0.123C



BETA=46.0 DEG. Y=0.2C

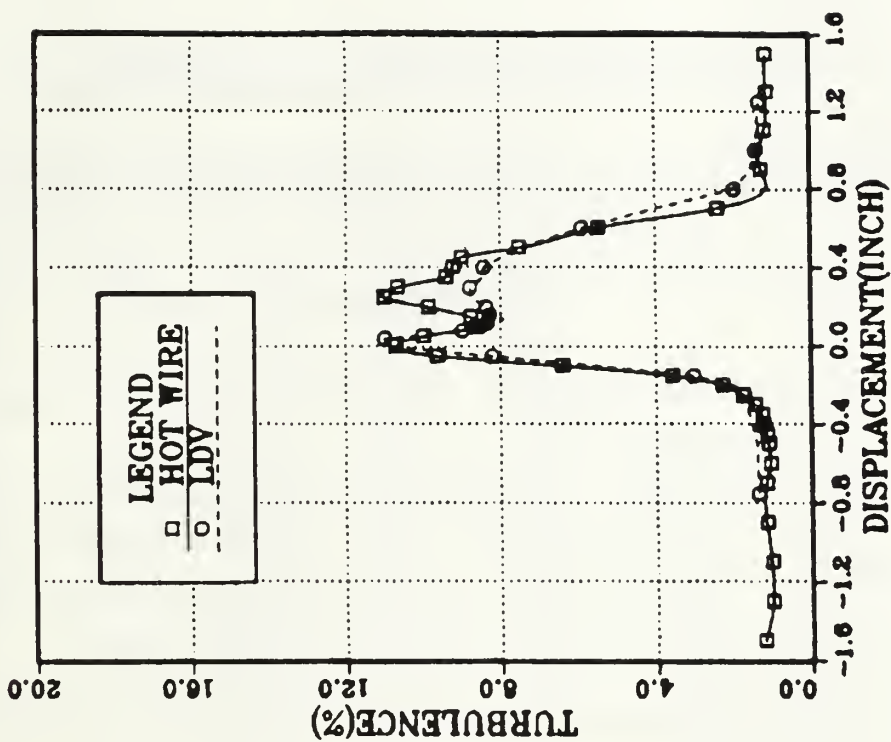


Figure 20. Wake Turbulence Comparison with LDV at  $\beta_1 = 46.0^\circ$

## VI. CONCLUSIONS AND RECOMMENDATIONS

From the program of hot-wire measurements and comparison with data obtained using a two component LDV system, the following conclusions were drawn:

a. The hardware and the software of the hot-wire system were verified for single channel operation with manual input of probe position. The software was not difficult to use.

b. The wake velocity distribution data agreed with LDV wake velocity to within the accuracy of the measurements.

c. Turbulence intensity data agreed well with LDV turbulence intensity data in spite of differences in the methods used by the two methods to calculate turbulence level. An exception to this general agreement was found in the center of the wake where the hot-wire recorded a reduced level of turbulence and the LDV did not.

d. Observations at  $\beta_1 = 48.0^\circ$  did not show any indication of impending stall. The blade suction side boundary layer appeared to be fully attached to the beginning of the trailing edge curvature.

The following recommendations are made:

a. Since the cascade wind tunnel temperature fluctuates somewhat, particularly early in a run, an alternate calibration procedure should be considered. Optimunly, the hot-wire needs to be in an environment in which the temperature does not change at all during the calibration. Temperature fluctuations are not a problem while measurements are being made.

b. Effort should be made to provide positive seals on the moving sections of the cascade to eliminate the need for extensive taping. The elimination of leaks is critical in obtaining proper cascade flow conditions.

c. A computer-controlled automatic traverse unit would greatly improve the accuracy in specifying probe displacement and also speed the process of data acquisition.



# APPENDIX A. TABULATED REDUCED DATA

Table 5. WAKE DISTRIBUTION DATA at  $\beta_1 = 40.0^\circ$ ,  $Y = 0.08c$

No	x(in.)	$V_1$ (m/s)	$V_2$ (m/s)	X	$T_{int.}$ (%)
1	-1.500	78.131	67.940	0.87	1.17
2	-1.300	78.131	67.290	0.86	1.26
3	-1.100	78.131	67.210	0.86	1.20
4	-0.900	78.131	66.950	0.86	1.20
5	-0.700	78.131	67.020	0.86	1.24
6	-0.600	78.131	66.730	0.85	1.18
7	-0.500	77.641	66.690	0.86	1.30
8	-0.450	77.641	66.450	0.86	1.27
9	-0.400	77.641	66.380	0.85	1.28
10	-0.350	77.641	66.620	0.86	1.33
11	-0.300	77.641	66.330	0.85	1.42
12	-0.250	77.641	65.690	0.85	1.47
13	-0.200	77.641	65.830	0.85	2.19
14	-0.150	77.641	63.210	0.81	4.57
15	-0.100	77.641	50.900	0.66	8.43
16	-0.050	77.641	33.140	0.43	10.22
17	0.000	77.641	17.540	0.23	9.26
18	0.050	77.641	13.910	0.18	9.65
19	0.100	77.641	24.540	0.32	9.68
20	0.150	76.153	40.100	0.53	8.01
21	0.200	76.153	50.500	0.66	6.21
22	0.250	76.153	60.120	0.79	3.55
23	0.300	76.153	63.030	0.83	1.62
24	0.350	76.153	63.760	0.84	1.41
25	0.400	76.153	63.950	0.84	1.34
26	0.450	76.153	63.940	0.84	1.14
27	0.500	76.153	64.080	0.84	1.20
28	0.600	76.153	63.830	0.84	1.20
29	0.700	76.153	64.250	0.84	1.15
30	0.900	76.153	63.860	0.84	1.20
31	1.100	76.153	64.120	0.84	1.19
32	1.300	76.153	63.910	0.84	1.24
33	1.500	76.153	63.520	0.83	1.27



Table 6. WAKE DISTRIBUTION DATA at  $\beta_1 = 40.0^\circ$ ,  $\Gamma = 0.123c$

No	x(in.)	$V_1$ (m/s)	$V_2$ (m/s)	X	$T_{int.}$ (%)
1	-1.500	76.652	65.830	0.86	1.22
2	-1.300	76.652	65.540	0.86	1.33
3	-1.100	76.652	65.280	0.85	1.25
4	-0.900	76.153	64.580	0.85	1.28
5	-0.700	76.153	64.530	0.85	1.24
6	-0.600	76.153	64.890	0.85	1.27
7	-0.500	76.153	64.370	0.85	1.23
8	-0.450	76.153	64.420	0.85	1.14
9	-0.400	76.153	64.520	0.85	1.20
10	-0.350	76.153	64.480	0.85	1.26
11	-0.300	76.153	64.140	0.84	1.38
12	-0.250	76.153	64.180	0.84	1.59
13	-0.200	76.153	64.340	0.84	1.95
14	-0.150	76.153	64.110	0.84	2.90
15	-0.100	76.153	60.050	0.79	6.02
16	-0.050	76.153	47.460	0.62	9.28
17	0.000	76.153	35.180	0.46	9.82
18	0.050	76.153	24.230	0.32	8.45
19	0.100	76.153	23.150	0.30	9.53
20	0.150	76.153	32.690	0.43	9.42
21	0.200	76.153	45.270	0.59	7.95
22	0.250	76.153	57.020	0.75	5.54
23	0.300	76.153	62.920	0.83	2.71
24	0.350	76.153	64.450	0.85	1.69
25	0.400	75.902	64.100	0.84	1.36
26	0.450	75.902	64.160	0.85	1.28
27	0.500	75.902	64.550	0.85	1.30
28	0.600	75.902	64.530	0.85	1.23
29	0.700	75.902	64.620	0.85	1.21
30	0.900	75.902	64.640	0.85	1.20
31	1.100	75.902	64.680	0.85	1.12
32	1.300	75.902	64.690	0.85	1.21
33	1.500	75.902	64.500	0.85	1.25

Table 7. WAKE DISTRIBUTION DATA at  $\beta_1 = 40.0^\circ$ ,  $Y = 0.2c$

No	x(in.)	$V_1(\text{m/s})$	$V_2(\text{m/s})$	X	$T_{int.} (\%)$
1	-1.500	76.403	64.450	0.84	1.13
2	-1.300	76.403	64.500	0.84	1.22
3	-1.100	76.403	64.420	0.84	1.16
4	-0.900	76.403	64.230	0.84	1.24
5	-0.700	76.403	64.080	0.84	1.27
6	-0.600	76.403	64.140	0.84	1.17
7	-0.500	76.403	63.920	0.84	1.15
8	-0.450	76.403	63.930	0.84	1.14
9	-0.400	76.403	63.850	0.84	1.22
10	-0.350	76.403	63.520	0.83	1.32
11	-0.300	76.403	63.230	0.83	1.36
12	-0.250	76.403	62.910	0.82	1.73
13	-0.200	76.403	63.190	0.83	2.16
14	-0.150	76.403	63.010	0.82	3.08
15	-0.100	76.403	60.260	0.79	6.04
16	-0.050	76.403	54.260	0.71	8.27
17	0.000	76.403	45.730	0.60	9.42
18	0.050	76.403	35.740	0.47	9.14
19	0.100	76.403	30.540	0.40	7.61
20	0.150	76.403	34.930	0.46	8.36
21	0.200	76.403	42.460	0.56	8.96
22	0.250	76.403	52.070	0.68	7.59
23	0.300	76.403	60.360	0.79	4.72
24	0.350	76.403	62.740	0.82	2.05
25	0.400	75.902	63.120	0.83	1.50
26	0.450	75.902	63.200	0.83	1.38
27	0.500	75.902	63.000	0.83	1.36
28	0.600	75.902	62.890	0.83	1.23
29	0.700	75.902	63.040	0.83	1.22
30	0.900	75.902	63.110	0.83	1.22
31	1.100	75.902	63.190	0.83	1.20
32	1.300	75.902	63.230	0.83	1.34
33	1.500	75.902	62.890	0.83	1.38

**Table 8. WAKE DISTRIBUTION DATA at  $\beta_1 = 46.0^\circ$ ,  $Y = 0.08c$**

No	x(in.)	$V_1$ (m/s)	$V_2$ (m/s)	X	$T_{int.}$ (%)
1	-1.500	76.403	60.890	0.797	1.019
2	-1.300	76.403	60.760	0.795	1.031
3	-1.100	76.403	60.730	0.795	1.083
4	-0.900	76.403	60.820	0.796	0.990
5	-0.700	76.403	60.640	0.794	1.022
6	-0.600	76.403	60.940	0.798	1.039
7	-0.500	76.403	61.160	0.800	1.104
8	-0.450	76.403	60.730	0.795	1.071
9	-0.400	76.403	60.680	0.794	1.213
10	-0.350	76.403	60.550	0.793	1.293
11	-0.300	76.403	60.810	0.796	1.260
12	-0.250	76.403	61.020	0.799	1.380
13	-0.200	76.403	61.000	0.798	2.371
14	-0.150	76.403	57.350	0.751	5.340
15	-0.100	76.403	42.010	0.550	9.144
16	-0.050	76.403	21.610	0.283	9.493
17	0.000	76.403	9.972	0.131	8.645
18	0.050	76.403	8.681	0.114	8.865
19	0.100	76.403	13.730	0.180	10.598
20	0.150	76.403	19.830	0.260	11.016
21	0.200	76.403	25.210	0.330	10.275
22	0.250	76.403	30.370	0.397	9.974
23	0.300	76.403	38.070	0.498	9.189
24	0.350	76.403	42.490	0.556	8.209
25	0.400	76.403	47.000	0.615	8.040
26	0.450	76.403	51.540	0.675	6.712
27	0.500	76.403	55.650	0.728	5.530
28	0.600	76.403	60.580	0.793	2.395
29	0.700	76.403	60.930	0.797	1.337
30	0.900	76.403	60.970	0.798	1.148
31	1.100	76.403	61.100	0.800	1.066
32	1.300	76.403	61.200	0.801	1.073
33	1.500	76.403	60.880	0.797	1.110

Table 9. WAKE DISTRIBUTION DATA at  $\beta_1 = 46.0^\circ$ ,  $Y = 0.123c$

No	x(in.)	$V_1$ (m/s)	$V_2$ (m/s)	X	$T_{int.}$ (%)
1	-1.500	78.860	62.050	0.787	1.140
2	-1.300	78.860	62.230	0.789	1.062
3	-1.100	77.395	62.020	0.801	1.035
4	-0.900	77.395	61.750	0.798	1.012
5	-0.700	77.395	61.350	0.793	1.004
6	-0.600	77.395	60.980	0.788	1.102
7	-0.500	77.395	60.950	0.788	1.046
8	-0.450	77.395	60.840	0.786	1.083
9	-0.400	77.395	60.910	0.787	1.185
10	-0.350	77.395	60.480	0.781	1.279
11	-0.300	77.395	60.430	0.781	1.379
12	-0.250	77.395	60.440	0.781	1.747
13	-0.200	77.395	60.710	0.784	2.353
14	-0.150	77.395	58.120	0.751	5.037
15	-0.100	77.395	47.730	0.617	9.150
16	-0.050	77.395	32.470	0.420	10.527
17	0.000	77.395	19.840	0.256	9.137
18	0.050	77.395	13.000	0.168	8.193
19	0.100	77.395	15.110	0.195	9.814
20	0.150	77.395	19.020	0.246	11.127
21	0.200	77.395	22.920	0.296	11.777
22	0.250	76.652	30.520	0.398	9.971
23	0.300	76.652	35.920	0.469	9.306
24	0.350	76.652	40.870	0.533	8.905
25	0.400	76.652	46.230	0.603	7.902
26	0.450	76.652	50.010	0.652	7.166
27	0.500	76.652	53.670	0.700	6.251
28	0.600	76.652	59.470	0.776	2.858
29	0.700	76.652	60.430	0.788	1.424
30	0.900	76.652	60.830	0.794	1.125
31	1.100	76.652	60.440	0.788	1.100
32	1.300	76.652	61.100	0.797	1.124
33	1.500	76.652	61.240	0.799	1.042

Table 10. WAKE DISTRIBUTION DATA at  $\beta_1 = 46.0^\circ$ ,  $Y = 0.2c$

No	x(in.)	$V_1$ (m/s)	$V_2$ (m/s)	X	$T_{int.}$ (%)
1	-1.500	78.860	62.830	0.797	1.224
2	-1.300	78.860	62.530	0.793	1.022
3	-1.100	78.860	62.990	0.799	1.043
4	-0.900	78.860	62.600	0.794	1.164
5	-0.700	78.860	62.990	0.799	1.173
6	-0.600	78.860	62.880	0.797	1.062
7	-0.500	78.860	62.770	0.796	1.102
8	-0.450	78.860	62.820	0.797	1.150
9	-0.400	78.860	62.640	0.794	1.264
10	-0.350	78.860	62.160	0.788	1.268
11	-0.300	78.860	62.980	0.799	1.440
12	-0.250	77.395	60.880	0.787	1.759
13	-0.200	77.395	60.970	0.788	2.276
14	-0.150	77.395	60.370	0.780	3.579
15	-0.100	77.395	53.130	0.686	6.401
16	-0.050	77.395	46.880	0.606	9.635
17	0.000	77.395	37.400	0.483	10.703
18	0.050	77.395	27.920	0.361	9.985
19	0.100	77.395	21.010	0.271	8.581
20	0.150	77.395	20.220	0.261	8.769
21	0.200	77.395	21.900	0.283	9.861
22	0.250	77.395	23.460	0.303	11.011
23	0.300	77.395	28.240	0.365	10.657
24	0.350	77.395	36.510	0.472	9.401
25	0.400	77.395	40.190	0.519	9.228
26	0.450	77.395	44.410	0.574	8.999
27	0.500	77.395	48.290	0.624	7.523
28	0.600	77.395	55.350	0.715	5.476
29	0.700	77.395	61.150	0.790	2.391
30	0.900	77.395	61.660	0.797	1.237
31	1.100	77.395	61.430	0.794	1.142
32	1.300	77.395	61.820	0.799	1.083
33	1.500	77.395	61.100	0.789	1.103

Table 11. WAKE DISTRIBUTION DATA at  $\beta_1 = 48.0^\circ$ ,  $Y = 0.08c$

No	x(in.)	$V_1(\text{m/s})$	$V_2(\text{m/s})$	X	$T_{int.} (\%)$
1	-1.300	76.901	66.740	0.87	1.17
2	-1.100	76.901	66.300	0.86	1.10
3	-0.800	76.901	66.510	0.86	1.06
4	-0.600	76.901	66.480	0.86	1.18
5	-0.500	76.901	66.220	0.86	1.18
6	-0.400	76.901	66.920	0.87	1.07
7	-0.300	76.901	66.970	0.87	1.23
8	-0.200	76.901	67.400	0.88	1.38
9	-0.150	76.901	67.180	0.87	1.82
10	-0.100	76.901	66.010	0.86	4.86
11	-0.050	76.901	52.630	0.68	10.75
12	0.000	76.901	29.120	0.38	12.83
13	0.050	76.901	13.670	0.18	10.16
14	0.100	76.901	10.010	0.13	10.42
15	0.150	76.901	11.420	0.15	11.78
16	0.200	76.901	14.760	0.19	12.17
17	0.250	76.901	18.460	0.24	13.55
18	0.300	76.901	23.980	0.31	13.85
19	0.350	76.901	27.940	0.36	13.15
20	0.400	76.901	34.820	0.45	13.06
21	0.450	76.901	37.560	0.49	13.33
22	0.500	76.901	43.130	0.56	12.10
23	0.550	76.901	47.730	0.62	11.16
24	0.600	76.901	52.470	0.68	11.09
25	0.650	76.901	55.280	0.72	10.27
26	0.700	76.901	58.350	0.76	9.01
27	0.800	76.901	64.620	0.84	5.49
28	0.900	76.901	67.020	0.87	2.93
29	1.000	76.901	67.260	0.87	1.76
30	1.100	76.901	67.190	0.87	1.38
31	1.200	76.901	66.380	0.86	1.29
32	1.300	76.901	66.580	0.87	1.25
33	1.500	76.901	66.620	0.87	1.26



Table 12. WAKE DISTRIBUTION DATA at  $\beta_1 = 48.0^\circ$ ,  $Y = 0.123c$

No	x(in.)	$V_1$ (m/s)	$V_2$ (m/s)	X	$T_{int.}$ (%)
1	-1.500	78.618	66.440	0.85	1.08
2	-1.300	78.618	66.630	0.85	1.07
3	-1.000	78.618	66.460	0.85	1.12
4	-0.800	78.131	66.450	0.85	1.10
5	-0.600	78.131	66.960	0.86	1.26
6	-0.500	78.131	66.390	0.85	1.16
7	-0.400	77.641	66.920	0.86	1.14
8	-0.350	77.641	66.890	0.86	1.25
9	-0.300	77.641	66.200	0.85	1.39
10	-0.250	77.641	66.660	0.86	1.53
11	-0.200	77.641	66.490	0.86	1.88
12	-0.150	77.641	66.640	0.86	2.96
13	-0.100	77.641	63.070	0.81	6.41
14	-0.050	77.641	49.360	0.64	11.82
15	0.000	77.641	32.540	0.42	13.02
16	0.050	77.641	17.970	0.23	10.53
17	0.100	77.641	13.890	0.18	9.89
18	0.200	77.641	15.200	0.20	11.21
19	0.250	77.641	16.860	0.22	12.44
20	0.300	77.641	21.010	0.27	13.34
21	0.350	77.641	24.720	0.32	12.87
22	0.400	77.641	30.090	0.39	12.92
23	0.450	77.641	34.500	0.44	13.09
24	0.500	77.641	38.280	0.49	12.02
25	0.550	77.641	43.930	0.57	11.43
26	0.600	77.641	46.810	0.60	11.69
27	0.700	77.641	55.460	0.71	9.97
28	0.800	77.641	62.810	0.81	7.02
29	0.900	77.641	66.350	0.85	3.41
30	1.000	77.641	66.280	0.85	2.15
31	1.100	77.641	66.300	0.85	1.55
32	1.300	77.641	66.500	0.86	1.59
33	1.500	77.641	66.790	0.86	1.55

Table 13. WAKE DISTRIBUTION DATA at  $\beta_1 = 48.0^\circ$ ,  $Y = 0.2c$

No	x(in.)	$V_1$ (m/s)	$V_2$ (m/s)	X	$T_{int.}$ (%)
1	-1.500	82.871	70.050	0.85	1.03
2	-1.300	82.871	70.050	0.85	1.04
3	-1.100	82.871	70.010	0.84	0.99
4	-0.900	82.871	69.790	0.84	1.08
5	-0.700	82.871	69.520	0.84	1.03
6	-0.600	82.640	69.330	0.84	1.06
7	-0.500	82.640	68.980	0.83	1.16
8	-0.450	82.640	68.530	0.83	1.15
9	-0.400	82.640	68.790	0.83	1.30
10	-0.350	82.640	68.580	0.83	1.34
11	-0.300	82.640	69.120	0.84	1.53
12	-0.250	82.640	68.800	0.83	1.94
13	-0.200	82.640	68.580	0.83	2.54
14	-0.150	82.640	67.670	0.82	4.55
15	-0.100	82.409	62.080	0.75	8.28
16	-0.050	82.409	53.550	0.65	10.85
17	0.000	82.409	40.640	0.49	11.21
18	0.050	82.409	30.630	0.37	10.99
19	0.100	82.409	23.230	0.28	10.46
20	0.150	82.409	19.820	0.24	11.14
21	0.200	82.177	20.350	0.25	11.53
22	0.250	82.177	24.280	0.30	12.45
23	0.300	82.177	27.240	0.33	12.26
24	0.350	82.177	32.210	0.39	12.70
25	0.400	82.177	36.740	0.45	11.15
26	0.450	82.177	38.890	0.47	11.91
27	0.500	82.177	42.810	0.52	11.03
28	0.600	82.177	50.830	0.62	9.74
29	0.700	82.177	58.040	0.71	8.68
30	0.800	82.177	65.470	0.80	5.68
31	1.000	82.177	69.120	0.84	1.81
32	1.200	82.177	68.700	0.84	1.20
33	1.400	82.177	68.850	0.84	1.20

## APPENDIX B. CALCULATION OF DIMENSIONLESS PARAMETERS

The inlet velocity was made dimensionless by dividing by total velocity  $V_t$  which is given by

$$V_t = \sqrt{2C_p T_t}$$

where  $T_t$  is the total temperature and  $C_p$  is the specific heat at constant pressure.

Then the dimensionless velocity  $X$  is given by;

$$X = \frac{V_1}{V_t}$$

The relationship between dimensionless velocity and temperature ratio is given for a perfect gas [Ref. 8].

$$\frac{T}{T_t} = 1 - X^2$$

Whereas, in terms of Mach number;

$$\frac{T}{T_t} = 1 - \frac{\gamma - 1}{2} M^2$$

Therefore, the relationship between Mach number and dimensionless velocity is

$$M^2 = \frac{2}{\gamma - 1} \left( \frac{X^2}{1 - X^2} \right)$$

The Reynold's number is given by

$$R_e = \frac{\rho V_1 C}{\mu}$$

where  $\rho$  is the density of the fluid calculated from inlet flow conditions using the perfect gas equation of state,

$V_1$  is the inlet flow velocity,

$C$  is the chord length of the blade,

$\mu$  is the viscosity.

## LIST OF REFERENCES

1. Hobbs, D.E. and Weingold, H.D., *Development of Controlled Diffusion Airfoils For Multistage Compressor Applications*, Journal of Engineering For Gas Turbines and Power, v. 106, pp. 271-278, April 1984.
2. Nasa Technical Memorandum 82763, *The Use of Optimization Techniques to Design Compressor Blading*, by N.L. Sanger, Lewis Research Center, Cleveland, Ohio, 1982.
3. Koyuncu, Y., *Report of Tests of A Compressor Configuration of Controlled Diffusion Blading*, M.S. Thesis, Naval Postgraduate School, Monterey, California, March 1984.
4. Sanger, N. L. and Shreeve, R. P., *Comparision of Calculated and Experimental Cascade Performance for Controlled Diffusion Compressor Stator Blading* , Journal of Turbomachinery, v.108, pp. 42-50, July 1986.
5. Dreon, J. W., *Controlled Diffusion Compressor Blade Wake Measurements*, M.S. Thesis, Naval Postgraduate School, Monterey, California, September 1986.
6. Elazar, Y., *A Mapping of the Flow Behavior in a Controlled Diffusion Compressor Cascade Using Laser Doppler Velocimetry and Preliminary Evaluation of Codes for the Prediction of Stall*, Ph.D. Dissertation, Naval Postgraduate School, Monterey, California, March 1988.
7. TSI Company, *IFA 100 Intelligent Flow Analyzer Instruction Manual* , 1983.
8. NPS Technical Report 57Sf73071A, *Calibration of Flow Nozzels Using Traversing Pitot-Static Probes*, by Shreeve, R. P., Naval Postgraduate School, Monterey, California.

## INITIAL DISTRIBUTION LIST

	No. Copies
1. Defense Technical Information Center Cameron Station Alexandria, VA 22304-6145	2
2. Library, Code 0142 Naval Postgraduate School Monterey, CA 93943-5002	2
3. Naval Air Systems Command Washington, D.C. 20361 Attention: Code AIR 931E	1
4. Naval Air Systems Command Washington, D.C. 20361 Attention: Code AIR 93D	1
5. Naval Air Systems Command Washington, D.C. 20361 Attention: Code AIR 5004	4
6. Office of Naval Research 800 N. Quincy Street Arlington, Virginia 22217 Attention: Dr. Jack Hansen	1
7. Commanding Officer Naval Air Propulsion Center Trenton, NJ 08628 Attention: G. Mangano, PE-31	1
8. Department Chairman, Code 67 Department of Aeronautics Naval Postgraduate School Monterey, CA 93943	1
9. Director, Turbopropulsion Laboratory, Code 67Sf Department of Aeronautics Naval Postgraduate School Monterey, CA 93943	10
10. Hıv.K.Komutanligi Ogretim ve Egitim Daire Bsk.ligi Bakanliklar-Ankara /TURKEY	1
11. Hava Harp Okulu Kutuphanesi Yesilyurt-ISTANBUL /TURKEY	1

- |     |  |   |
|-----|--|---|
| 12. | Istanbul Teknik Universitesi<br>Kutuphanesi<br>Istanbul-TURKEY | 1 |
| 13. | Bogazici Universitesi<br>Kutuphanesi<br>Istanbul-TURKEY        | 1 |
| 14. | Orta Dogu Teknik Universitesi<br>Kutuphanesi<br>Ankara-TURKEY  | 1 |
| 15. | Ugsm. Adem Baydar<br>Istanbul Cad. No 73/A<br>Konya-TURKEY     | 2 |



















The  
B2  
c. Thesis  
B2465  
c.1

Baydar  
Hot-wire measurements  
of compressor blade  
wakes in a cascade wind  
tunnel.

Thesis  
B2465  
c.1

Baydar  
Hot-wire measurements  
of compressor blade  
wakes in a cascade wind  
tunnel.



thesB2465

Hot-wire measurements of compressor blad



3 2768 000 78057 1  
DUDLEY KNOX LIBRARY